

**Design and Synthesis of New Porphyrin based
Covalent Organic Frameworks (COFs)
Containing Intramolecular H-Bonding for the
Enhancement of its Stability and Crystallinity**

A thesis submitted to

Indian Institute of Science Education and Research (IISER), Pune;
in partial fulfillment of the requirements for the
BS-MS Dual Degree Programme

By

Raya Rahul Kumar

(ID:20091062)

Thesis Supervisor

Dr. Rahul Banerjee,

Scientist,

CSIR-National Chemical Laboratory, Pune.



*Indian Institute of Science Education and Research (IISER),
Pashan, Pune, India 411008.*

Certificate

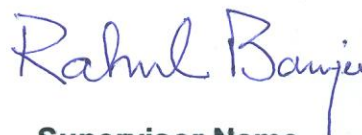
This is to certify that this thesis entitled "***Design and Synthesis of New Porphyrin based COF Containing Intramolecular H-Bonding for the Enhancement of its Stability and Crystallinity***" submitted towards the partial fulfillment of the BS-MS dual degree programme at the Indian Institute of Science Education and Research, Pune; represents work carried out by **Raya Rahul Kumar** under the supervision of **Dr. Rahul Banerjee**, Scientist, CSIR-National Chemical Laboratory, Pune; during the academic year 2013-2014. In this thesis, chapters are divided as:

Chapter 1: The introduction on porous COF materials, wherein the information regarding COFs is gathered from previously reported literature.

Chapter 2: This work is a reproduction of the published *Angew. Chem. Int. Ed.* **2013**, *52*, 13052 paper, wherein the data presented in the thesis are original.

Chapter 3: Completely unpublished and original data has been presented based on the intramolecular hydrogen bonding involving porphyrin based COFs, which will be published in future.

Date: 16th May 2014
Place: Pune




Supervisor Name

Dr. Rahul Banerjee,
Scientist,
CSIR-NCL, Pune.

DECLARATION

I hereby declare that the matter embodied in the report entitled Design and Synthesis of New Porphyrin based Covalent Organic Frameworks (COFs) Containing Intramolecular H-Bonding for the Enhancement of its Stability and Crystallinity are the results of innovations carried out by me at the National Chemical Laboratory-CSIR Under the supervision of Dr. Rahul Banerjee. And the same has not been submitted elsewhere for any other degree.

Date: 15 -05-2014
Place: pune


Raja Rahul Kumar
BS-MS Dual Degree Program,
IISER Pune.

Dedicate to All my family Members

Acknowledgments

This thesis has been kept on track and been seen through to completion with the support and encouragement of numerous people. At the end of my thesis, it is a pleasant task to express my thanks to all those who contributed in many ways to the success of this study and made it an unforgettable experience for me.

I wish to express my sincere and heartfelt sense of gratitude to my guide **Dr. Rahul Banerjee**, Scientist, Physical and Material Chemistry Division, CSIR-National Chemical Laboratory, Pune, for providing me an incredible opportunity to carry out my BS-MS 5th year project under his guidance, for his valuable advice and constant encouragement at every step of this project. I am thankful to my local supervisor **Dr. Nirmalya Ballav**, Assistant Professor, Department of Chemistry, IISER, Pune, for his guidance and support for my project.

I wish to express my sincere thanks to Dr. Sourav pal, Director, CSIR-NCL for having given an opportunity to carry out this work in this institute. I am extremely grateful to **Dr. K.N.Ganesh**, Director, IISER, Pune, for giving me the opportunity to work on a project and providing necessary response for the same.

I owe my sincere gratitude to Dr. Digambar Shinde, Dr. Gobinda Das, Dr. Jayshri, Sharath K, Pradip Pachfule, Chandan Dey, Tamas Panda, Arijit Mallick, Tanay Kundu, Subhadeep Saha, Suman Chandra, Harshitha, and B. A. Bikas Garai for supporting me with their guidance at my tenure in the lab.

I owe everything to my dear Mother, Father and Brothers, for their sincere encouragement and inspiration throughout my work and lifting me uphill this phase of life. Besides this, several people have knowingly and unknowingly helped me in the successful completion of these five years.

Raya Rahul Kumar

Abstract

Design and Synthesis of New Porphyrin based Covalent Organic Frameworks (COFs) Containing Intramolecular H-Bonding for the Enhancement of its Stability and Crystallinity

By

Raya Rahul Kumar

Covalent organic frameworks (COFs) represent an exciting new type of porous organic materials, which are ingeniously constructed with organic building units *via* strong covalent bonds. The well-defined crystalline porous structures together with tailored functionalities have offered the COF materials superior potential in diverse applications, such as gas storage, adsorption, optoelectricity, and catalysis. In this report, introduction of intermolecular O-H...N=C hydrogen bonding as an extra stabilizing factor, which helps to improve the crystallinity, and porosity of the porphyrin containing covalent organic frameworks (COFs) has been demonstrated. An improvement in the chemical stability of COFs in aqueous and acidic medium as a result of intermolecular hydrogen bonding is obtained.

Contents

Abstract	Vi
CHAPTER-1	
1. Brief Review on Covalent Organic Framework:	1
1.2. Design and synthesis	2
1.2.1 Dynamic covalent chemistry	2
1.2.2 Structure of building blocks	2
1.2.3 Synthesis of COF	3
1.2.3.1. Building units for synthesis of COFs	4
1.2.4 Synthetic methods for synthesis of COFs	5
1.2.4.1 Solvothermal synthesis	5
1.2.4.2 Ionothermal synthesis	6
1.2.4.3 Microwave synthesis	6
1.2.4.4 Room-temperature synthesis	6
1.3. Types of synthesized COFs	6
1.3.1 Boron-containing COFs	6
1.3.2 Triazine-based COFs (CTFs)	7
1.3.3 Imine-based COFs	8
1.4. Characterization of COFs	8
1.5. Applications of COFs	9
1.5.1 Gas Storage	9
1.5.1.1. H ₂ Storage	9
1.5.1.2. Methane storage	9
1.5.1.3. Carbon dioxide storage	10
1.5.1.4 Ammonia storage	10
1.5.2. Photoelectric applications	12
1.5.3. Catalysis	13

CHAPTER-2

2. Porphyrin based COFs	15
2.1. Introduction	15
2.2 Applications of porphyrin based COFs	15
2.3 Problem in Porphyrin based COFs	16
2.4 Synthesis of DhaTph containing intramolecular H-Bonding.	17
2.4.1.1 Synthesis of 5,10,15,20-Tetrakis(4-aminophenyl)-21 <i>H</i> ,23 <i>H</i> -porphine (Tph)	17
2.4.2.2. Synthesis of 2,5-Dihydroxy-1,4-benzenedicarboxaldehyde	18
2.4.3.1. Synthesis of DhaTph	19
2.5. Characterization of DhaTph	20
2.5.1 FT-IR of DhaTph	20
2.5.2 PXRD Pattern of DhaTph	21
2.5.3 Solid state ¹³ C-NMR	21
2.2.5.4. Gas adsorption of DhaTph	22
2.2.5.5. SEM and TEM of DhaTph	23
2.2.5.6 TGA of DhaTph	24

CHAPTER-3

3. New Porphyrin based COFs containing intramolecular: H-Bonding for Enhancement of stability and crystallinity	25
3.1 Introduction	25
3.2 Present Work	25
3.2.1 Synthesis of 2,3-dihydroxy-1,4-benzenedicarboxaldehyde	25
3.2.3.2. Synthesis of 2,3-dihydroxy-1,4-benzenedicarboxaldehyde	26
3.2.4. Synthesis of 1,2-DhaTph and 1,2-DmaTph	26
3.2.4.1. Synthesis of 1,2-DhaTph and 1,2-DmaTph	27
3.2.5. Characterization of 1,2-DhaTph	28
3.2.5.1 FT-IR of 1,2-DhaTph and 1,2-DmaTph	28
3.2.5.2 PXRD Pattern of 1,2-DhaTph and 1,2-DmaTph	28
3.2.5.3 Solid state ¹³ C-NMR	29
3.2.5.4. Gas adsorption of 1,2-DhaTph and 1,2-DmaTph	30

3.2.5.5. SEM and TEM of 1,2-DhaTph and 1,2-DmaTph	31
3.2.5.6 TGA of 1,2-DhaTph and 1,2-DmaTph	32
3.2.6 Stability test of 1,2-DhaTph and 1,2-DmaTph	33
Conclusion	35
Future plan	36
References	36
Poster on COFs	39

Chapter I. Brief Review on Covalent Organic Framework:

Past few decades, Due to the interest in the field of nanoporous materials has grown tremendously because of their outstanding performance and broad applications like gas storage, gas separation, catalysis, super hydrophobic interfaces, energy storage, energy conversion, and optoelectronics. Researchers have found new ideas to prepare a wide variety of porous materials. Since last few years due to the increased interest in vehicular onboard storage systems, materials which exhibit high surface areas and low densities are in great demand. Covalent organic frameworks (COFs) (**Figure 1**) are of particular interest because they are a class of crystalline porous polymers which are completely organic composition, not only lacks metal ions and clusters, but also involves the incorporation of relatively light elements such as H, C, O, N, B and Si.¹

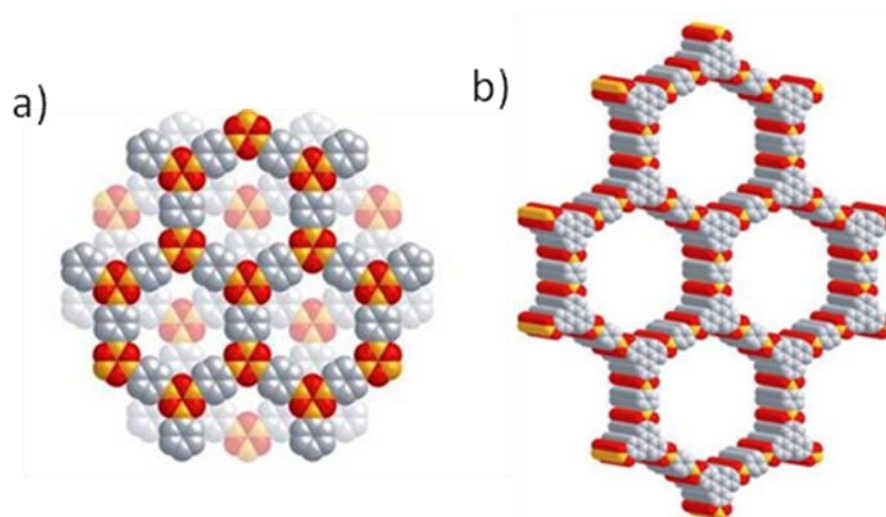


Figure 1: Structural representations of (a) COF-1 and (b) COF-5 based on powder diffraction and modelling projected along their *c* axes (H atoms are omitted).² (Reprinted with permission from Ref. 2. Copyright 2014 AAAS).

COFs also maintain the desirable thermal stability, and high porosity seen in other porous materials. COFs were first discovered in 2005 by Omar M. Yaghi and coworkers. The compositions of COFs are lighter elements, so they have very low density and could be utilized for gas storage effectively. Application of COFs as semiconducting and photoconductive device were also been explored because some

COFs have well aligned π - π stacked architecture. Researchers considered that reversibility in covalent bond formation during synthesis is required for the successful crystallization COFs. This is essential to identify their specific structural details such as space group, atomic positions, 2D and 3D architecture, etc.

1.2. Design and synthesis

1.2.1. Dynamic covalent chemistry:

Generally the organic polymers and polymeric materials are synthesized by kinetically controlled reactions, which irreversible form covalent bonds. Crystallization of linked organic polymers into solids using irreversible reactions is difficult. In contrast, dynamic covalent chemistry (DCC) leads to the reversible formation of covalent bonds, which can be formed, broken, and reformed. Therefore, unlike conventional covalent bond formation, DCC is thermodynamically controlled and thus offers reversible reaction systems with “error checking” and “proof-reading” characteristics, leading to the formation of the most thermodynamically stable structures. By using the DCC concept for the construction of COFs, the polymer skeleton formation occurs alongside the crystallization process, while the self-healing feedback reduces the incidence of structural defects and assists in the formation of an ordered structure. As a result, the final COF product possesses an ordered crystalline structure with high thermodynamic stability.

Two key issues that must be considered in the design and synthesis of COFs to achieve thermodynamic control in reversible reactions:

1. Structure of the building blocks, and
2. Synthetic method, including the reaction type and reaction conditions.

1.2.2 Structure of building blocks:

COFs are architecturally designed through reticular synthesis, which is a conceptual approach that uses secondary building blocks for the assembly of ordered predetermined structures. The four main types of building blocks include C_2 , C_3 , C_4 and Td that are named based on the directional symmetry of their reactive groups (**Figure**

2).^{3,4} All the building blocks are composed of arenes that have discrete bonding directions to guarantee a rigid framework. In order to ensure the formation of a crystalline, ordered framework, dynamic covalent chemical (DCC) reactions are utilized when combining these building blocks.

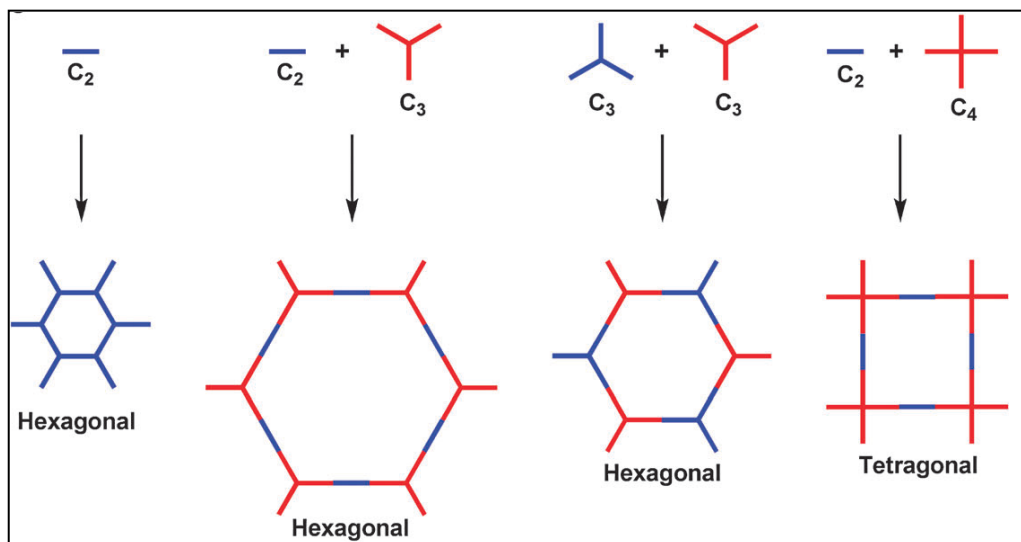


Figure 2: The combination of building blocks with different geometries to design COFs. (Reprinted with permission from Ref. 5. Copyright 2014 RSC).

1.2.3. Synthesis of COF:

The first covalent organic framework, COF-1, exhibited a 2-D honeycomb structure and was synthesized through the self- condensation of 1,4-benzene diboronic acid (BDDBA) (**Figure 3**) by Yaghi O.M and Co-workers.

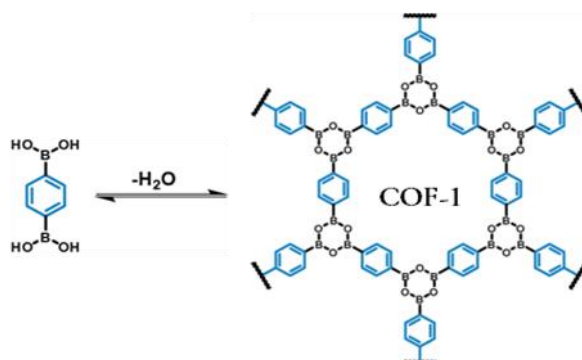


Figure 3: structure of COF-1 (Reprinted with permission from ref. 2 Copyright 2014 AAAS.).

1.2.3.1. Building units for synthesis of COFs:

For the synthesis of Covalent Organic frameworks (COFs) and for the efficient construction of porous structure, building units or linkers (**Figure 4**) with rigid aromatic moieties are preferable. And the linking groups formed with the given linkers or building units are boroxines, triazines, imines, or hydrazones, which are all rigid with a planar geometry. Using these building units researchers start synthesizing COFs by using different synthetic methods.

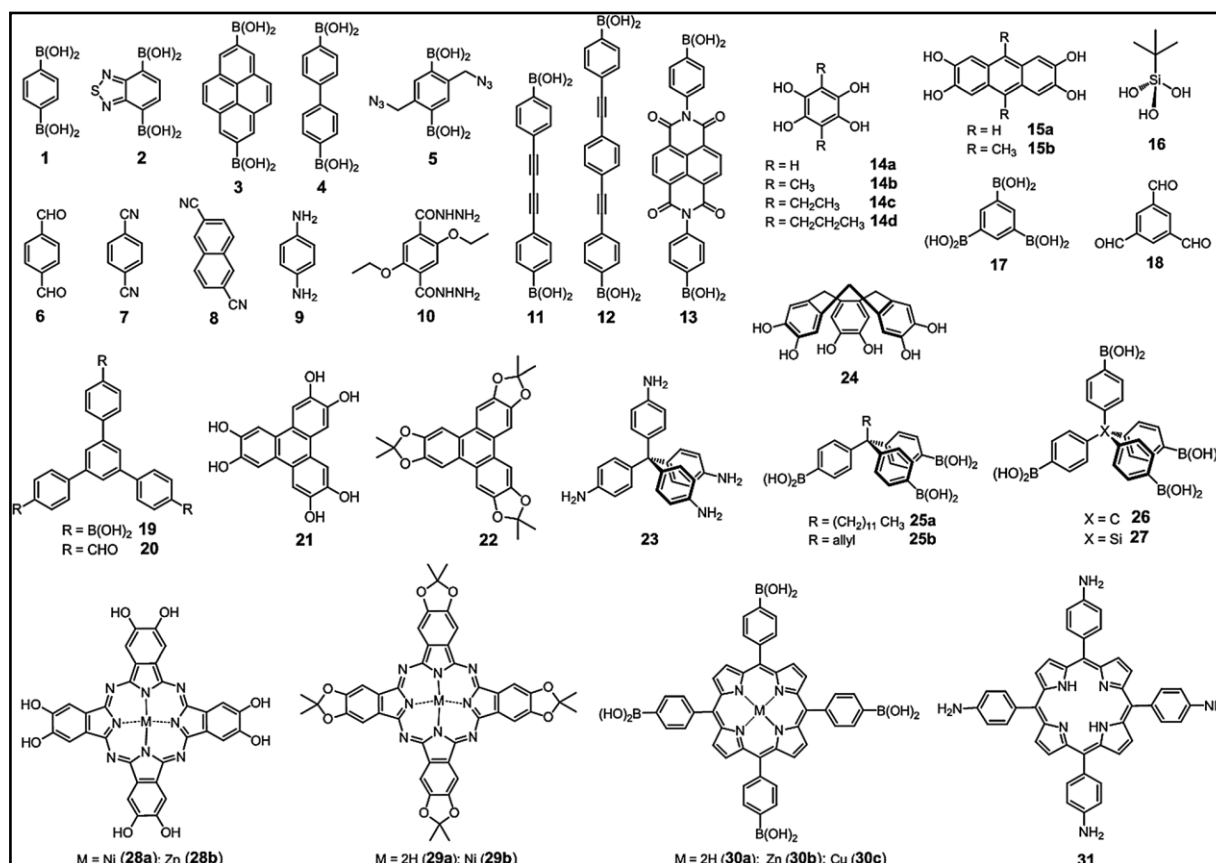


Figure 4: Building units that have been successfully utilized for the synthesis of COFs.

(Reprinted with permission from Ref. 11 Copyright 2014 RSC).

1.2.4. Synthetic methods for synthesis of COFs:

1.2.4.1 Solvothermal synthesis:

In the solvothermal technique reactants are dissolved in appropriate solvent in a Pyrex tube and degassed *via* several freeze-pump-thaw cycles. Then tube was sealed and heated to a required temperature for 72 hrs. The precipitate is collected, washed with suitable solvents several times, and dried under vacuum to get the final COF product as solid powder. Before selecting the reaction media conditions the major Issues like reaction rate, solubility, crystal nucleation, crystal growth rate, and 'self-healing' structure are important points to consider. Here we have given example of HHTP and PBBA mixed with mesitylene/dioxane was puted in pyrex tube at 90 °C for 72 h (**Figure 5**).

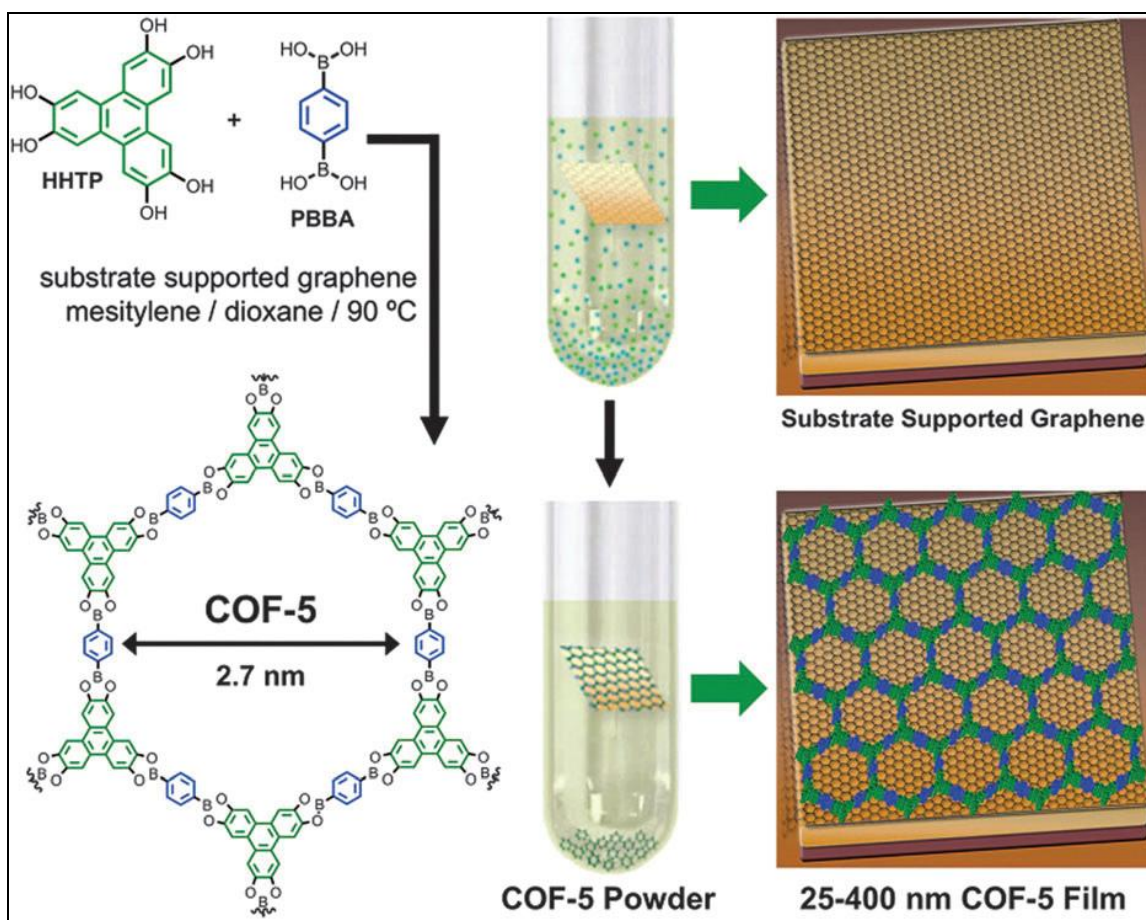


Figure 5: Solvothermal synthesis of 21 (HHTP) and 1 (PBBA) on a single-layer graphene surface, affording COF-5 as the film on the graphene surface and as the powder precipitated around the bottom of the tube.⁶ (Reprinted with permission from Ref. 6. Copyright 2014 AAAS).

1.2.4.2. Ionothermal synthesis:

Thomas and co-workers exploited the ionothermal synthesis method to produce crystalline porous COF-CTFs.^{7,8} The cyclotrimerization of aromatic nitrile building units (Figure 7c, 1,4-dicyanobenzene 7) in molten ZnCl₂ at 400°C affords crystalline conjugated CTFs with robust chemical and thermal stabilities. ZnCl₂ acts as both the solvent and the catalyst for the trimerization reaction, which seems to be partially reversible. However, such harsh reaction conditions limit the building block availability. Most synthesized CTFs are amorphous materials that lack long-range molecular order.

1.2.4.3, Microwave synthesis:

Cooper and co-workers synthesize boronate ester linked (Figure 6) COFs using Microwave technique.^{9,10} COF-5 was synthesized using microwave technique in which the reaction mixture of COF was sealed in a glass microwave tube under nitrogen and heated by microwave irradiation at 100 °C with stirring for 60 min at a power of 200W using a CEM S-Class Explorer™ 96-position microwave reactor with digital camera attachment.

1.2.4.4 Room-temperature synthesis:

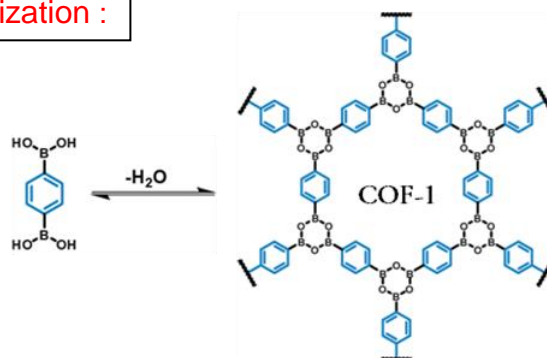
Recently W. Wang group put forward their step into the new methodology in COF synthesis, which is room temperature COF. Imine-based COFs could be facilely synthesized at room temperature and ambient atmosphere.¹¹ By avoiding both the use of sealed vessels and the difficulty in controlling different synthetic parameters, this method makes bulk production of the COF materials possible. This method is still under investigation.

1.3. Types of synthesized COFs:

So far there are different types of COFs were synthesized using building units like boron containing COFs, triazine based COFs, and imine based COFs.

1.3.1 Boron-containing COFs:

a: Boronic acid Trimerization :



b: Boronate ester Formation

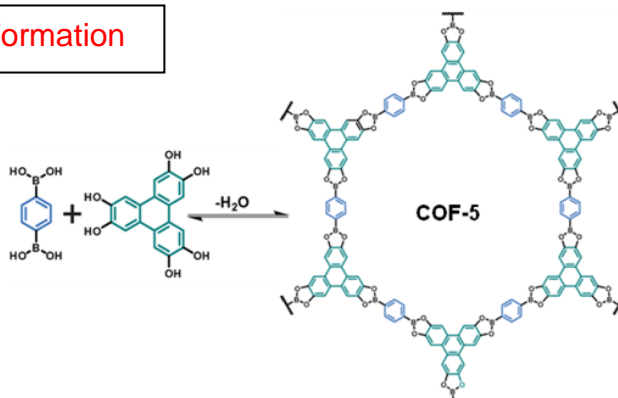


Figure 6: Synthesis of boron-containing COFs. a) Boronic acid trimerization (COF-1). and b) boronate ester formation(COF-5). (Reprinted with permission from Ref. 2 Copyright 2014 AAAS).

1.3.2 Triazine-based COFs (CTFs):

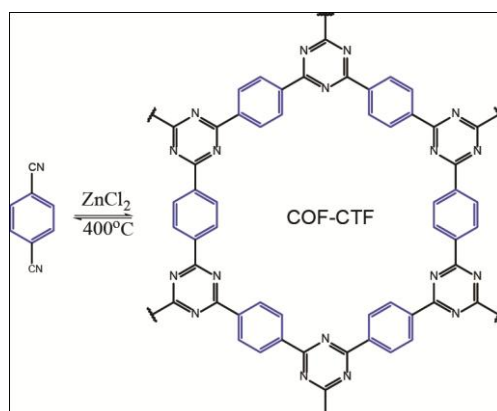


Figure 7: synthesis of triazine-based COFs, c) Trimerization of nitrile (COF-CTF). (Reprinted with permission from Ref. 21. Copyright 2014 Angew. Chem. Int. Ed.).

1.3.3 Imine-based COFs:

d: Schiff Base Reaction :

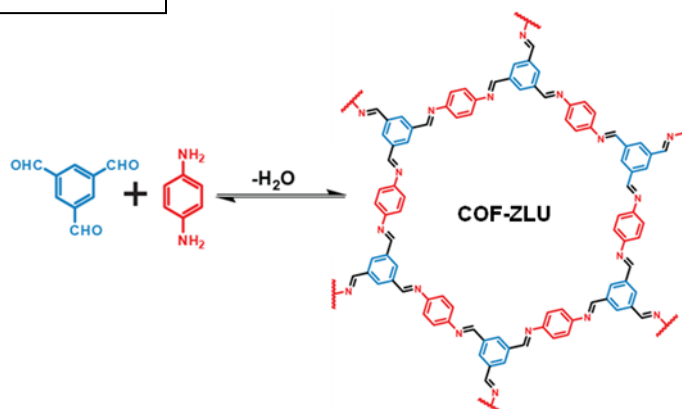


Figure 8: Synthesis of Imine-based COFs. d) Schiff base reaction. (Reprinted with permission from Ref. 22. Copyright 2014 J.Am.Chem. Soc.).

1.4. Characterization of COFs

The main concerns for characterizing COFs include the structural regularity, atomic connectivity, porosity, and morphology.

To characterize the COFs we use following techniques:

1. Powder X-ray Diffraction (PXRD).
2. Fourier transform infrared spectroscopy (FTIR).
3. Solid state ^{13}C NMR
4. Transmission electron microscope (TEM).
5. Scanning electron microscope (SEM)
6. Thermogravimetric analysis (TGA).
7. The surface area of the COFs calculated with the application of the Brunauer–Emmett–Teller (BET) model.
8. The NLDFT model was used to study the pore size distributions.
9. X-ray photoelectron spectroscopy (XPS) - helpful to investigate the state of metal ions incorporated into the COF materials.

Based on the classical molecular modeling method, computational modeling of the COF materials has attracted intense interest recently.¹² Most of the theoretical studies focus on the structural modeling of the COF materials, some of which deal further with the property prediction, such as the capability of COFs for hydrogen storage.^{12,13,14} The theoretical investigations have provided important information for characterization and application of COF materials in a predictive way.

1.5. Applications of COFs

Based on the design principles described above, a diversity of functional COF materials with tailored functionalities could be obtained. With tunable chemical and physical properties, these COF materials are new candidates for further applications, such as in gas storage, photoelectricity, and catalysis. This section summarizes the application progress of functional COF materials.

1.5.1 Gas Storage

1.5.1.1. Hydrogen (H₂) Storage:

The need for the reduction of air pollution and the increasing demands for energy have led to the search of new and clean energy sources. Due to its clean combustion and high chemical energy density, hydrogen has been pursued as an ideal substitute for traditional fossil fuels, especially in the automotive applications. For commercial use of hydrogen as a power source, efficient and safe storage of hydrogen is one of the main bottlenecks. Accordingly, a large number of studies have focused on the hydrogen storage with porous materials **Table 1**. The possibility of applying COF materials for hydrogen storage has also been pursued recently.

1.5.1.2. Methane (CH₄) storage:

As the main component of natural gas, methane is abundant and inexpensive in comparison with conventional fossil fuels. The current US DOE target for methane storage is 180 (v/v) at 35 bar and 298 K. In order to put methane into driving automobiles in a practical manner, effective and safe storage systems need to be developed. Accordingly, the capability of methane storage in certain COF materials has

been examined **Table 1.**^{15,16,17} Analogous to the cases of hydrogen storage, the capacities of methane storage in 3D COFs are higher than those of 2D COFs.

1.5.1.3. Carbon dioxide (CO₂) storage:

Nowadays, carbon dioxide emitting from the combustion of fossil fuels is thought to be a major contribution to the global warming. Therefore, how to efficiently capture and store carbon dioxide is an urgent issue for research.¹⁸ The storage of CO₂ has been extensively studied using a wide range of porous materials, such as porous carbons, silicas, and MOFs. The use of COF materials as the storage media has also been attempted.

Table 1: Systematic representation of Hydrogen, Methane, and Carbon dioxide uptakes of different COFs. (Reprinted with permission from ref. 11 Copyright 2014 RSC).

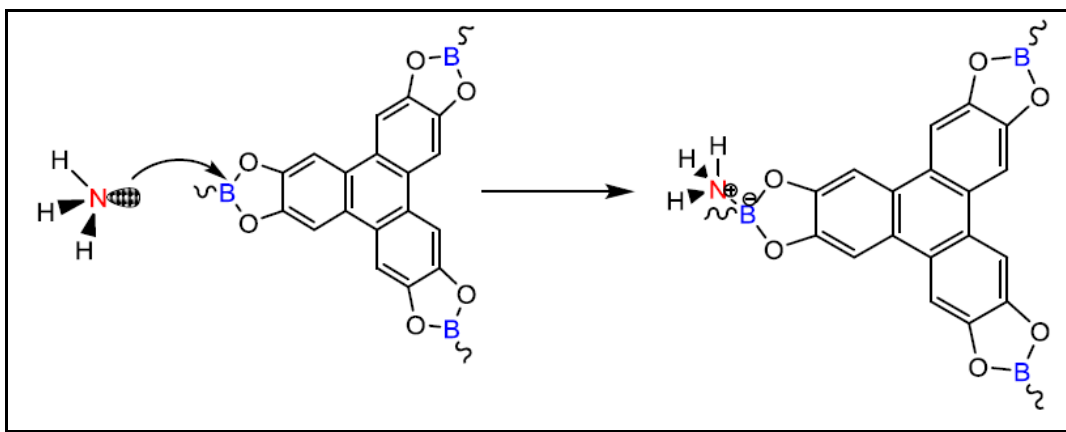
Material	BET surface area (m ² g ⁻¹)	Pore volume (V _p , cm ³ g ⁻¹)	H ₂ uptake ^a (wt%)	CH ₄ uptake ^c (mg g ⁻¹)	CO ₂ uptake ^d (mg g ⁻¹)
COF-1	750	0.30	1.48 ^b	40	230
COF-5	1670	1.07	3.58 ^b	89	870
COF-6	750	0.32	2.26 ^b	65	310
COF-8	1350	0.69	3.50 ^b	87	630
COF-10	1760	1.44	3.92 ^b	80	1010
COF-102	3620	1.55	7.24 ^b	187	1200
COF-103	3530	1.54	7.05 ^b	175	1190
COF-1	628	0.36	1.28 (1 bar)	—	—
COF-11Å	105	0.05	1.22 (1 bar)	—	—
COF-14Å	805	0.41	1.23 (1 bar)	—	—
COF-16Å	753	0.39	1.40 (1 bar)	—	—
COF-18Å	1263	0.69	1.55 (1 bar)	—	—
CTC-COF	1710	1.03	1.12 (1.05 bar)	—	—

^a H₂ uptake measured at 77 K. ^b H₂ uptake at saturation. ^c CH₄ uptake at 35 bar and 298 K. ^d CO₂ uptake at 55 bar and 298 K.

1.5.1.4. Ammonia (NH₃) storage:

Ammonia is widely used in industrial applications, such as in the production of nitrogen fertilizers. For commercial transportation and application, compressed liquid ammonia is often needed. However, the liquid ammonia is difficult to handle due to its toxicity and corrosiveness. Efficient and scalable storage of ammonia in adsorbents is, therefore, a practical way to solve this problem. Recently, Yaghi and co-workers reported that a boron containing COF, COF-10, has exceptionally high ammonia uptake in comparison with other porous materials. The total ammonia uptake capacity of COF-10 is 15 mol kg⁻¹ at 298 K and 1 bar, which is the highest among the porous materials reported, such as

Amberlyst 15 (11 mol kg^{-1}), zeolite 13X (9 mol kg^{-1}), and MCM-41 (7.9 mol kg^{-1}). Moreover, the ammonia uptake of COF-10 can be released and re-adsorbed in a reversible manner with a slight reduction (4.5%) in the total uptake capacity (**Figure 9**). The layered morphology of COF-10 was found disrupted during the adsorption cycles, but the atomic connectivity and periodicity are well maintained. The exceptionally high uptake of ammonia in COF-10 was explained by the formation of a classical ammonia–borane coordination bond (**Scheme1**). This research represents a nice example of applying COF materials in functional applications.



Scheme 1: The proposed ammonia-boron interaction upon the adsorption of ammonia on COF-10.¹⁹ (Reprinted with permission from ref. 19 Copyright 2014 Nat.Chem.)

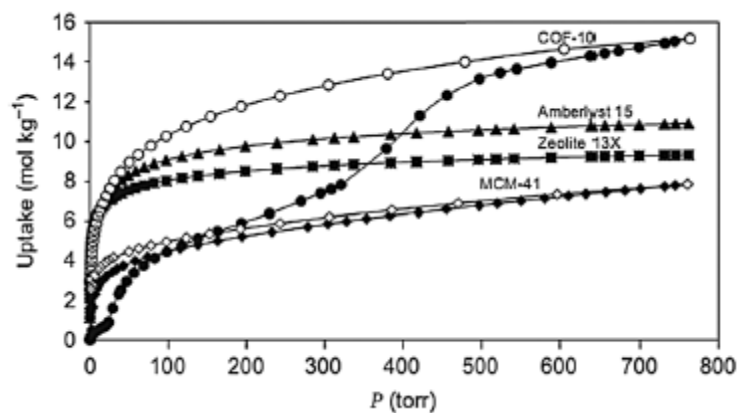


Figure 9: Ammonia uptakes in COF-10 and in other porous materials.¹⁹ (Reprinted with permission from Ref. 19. Copyright 2014 Nat. Chem.).

1.5.2. Photoelectric applications:

With certain photoelectric moieties embedded into the well defined framework, functional COF materials could possess unique optical and electrical properties. **PPy-COF** was obtained via the self-condensation of pyrene-2,7-diboronic acid (PDBA, 21),²⁰ while the TP-COF was obtained via the co-condensation of 2,3,6,7,10,11-hexahydroxytriphenylene (HHTP, 3) and PDBA 21 (Figure 10(3)).²¹ TP-COF is highly luminescent with a capacity of harvesting photons from ultraviolet to visible regions. Moreover, TP-COF exhibits the p-type semiconductive characters due to the eclipsed arrangement of triphenylene and pyrene units. Similarly, with the eclipsed alignment of polypyrene in the framework, PPy-COF shows a fluorescence shift comparable to the PDBA solids (Figure 10(1.2)).²⁰ PPy-COF is electrically conductive, revealing photoconductivity with a quick response to light irradiation (Figure 10(3)).²¹

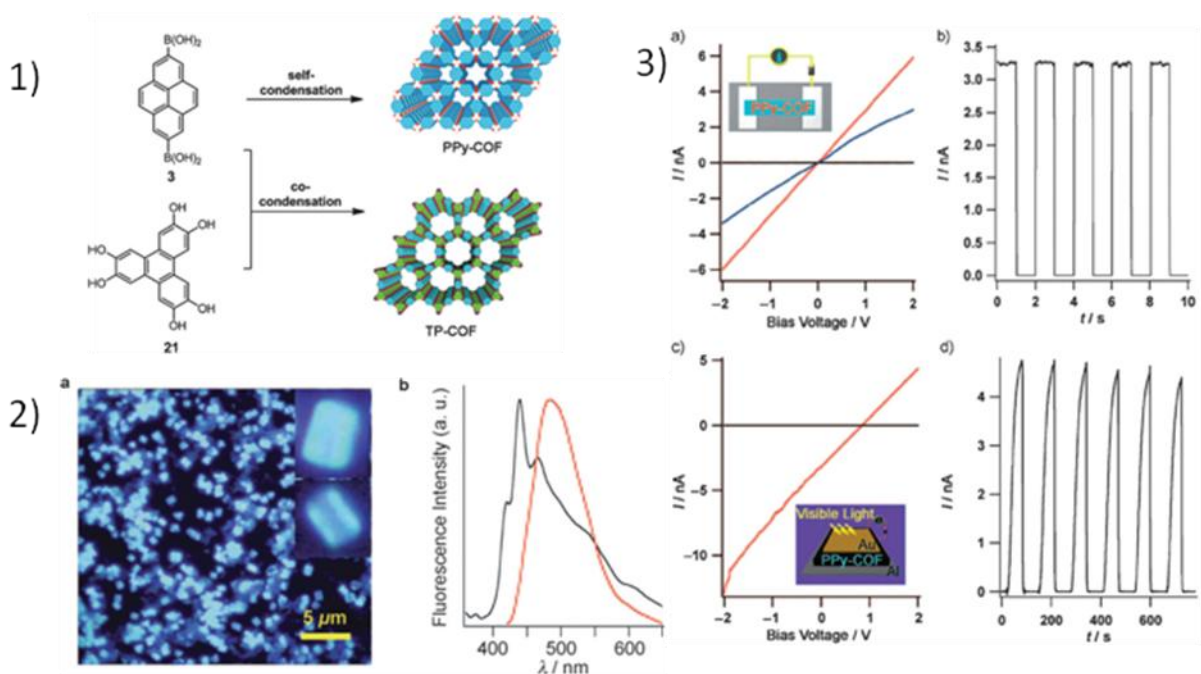


Figure 10: 1. Building units and extended structures of PPy-COF and TP-COF; 2. (a) Fluorescence microscopic image of PPy-COF (inset: enlargement of individual cubes) and (b) normalized fluorescence spectra of PPy-COF (red) and PDBA 21 (black) upon the excitation at 414 nm at 25 °C; 3. (a) I–V profile of PPy-COF between two Pt electrodes (black: without PPy-COF; blue: with PPy-COF; red: with iodine-doped PPy-COF). (b) Electric current with the bias voltage (2 V) on–off. (c) I–V profile of PPy-COF between sandwich type Al/Au electrodes (black:

without light irradiation; red: with light irradiation). (d) Photocurrent response with the light on–off. (Reprinted with permission from Ref. 20, 21. Copyright 2014 Angew. Chem. Int. Ed. and small).

1.5.3. Catalysis:

The functional COF materials possess high potentials as efficient and robust catalysts. As the cases of other porous solids, suitable COF candidates for catalytic applications should incorporate robust catalytic sites and possess high stability to thermal treatments, water, and most of the organic solvents. Furthermore, the easy accessibility to the catalytic sites and the efficient mass transport inside the porous catalyst should also be guaranteed for the ideal catalytic performance. Recently, researchers realized the first application of COF materials for highly efficient catalysis (Figure 11).²²

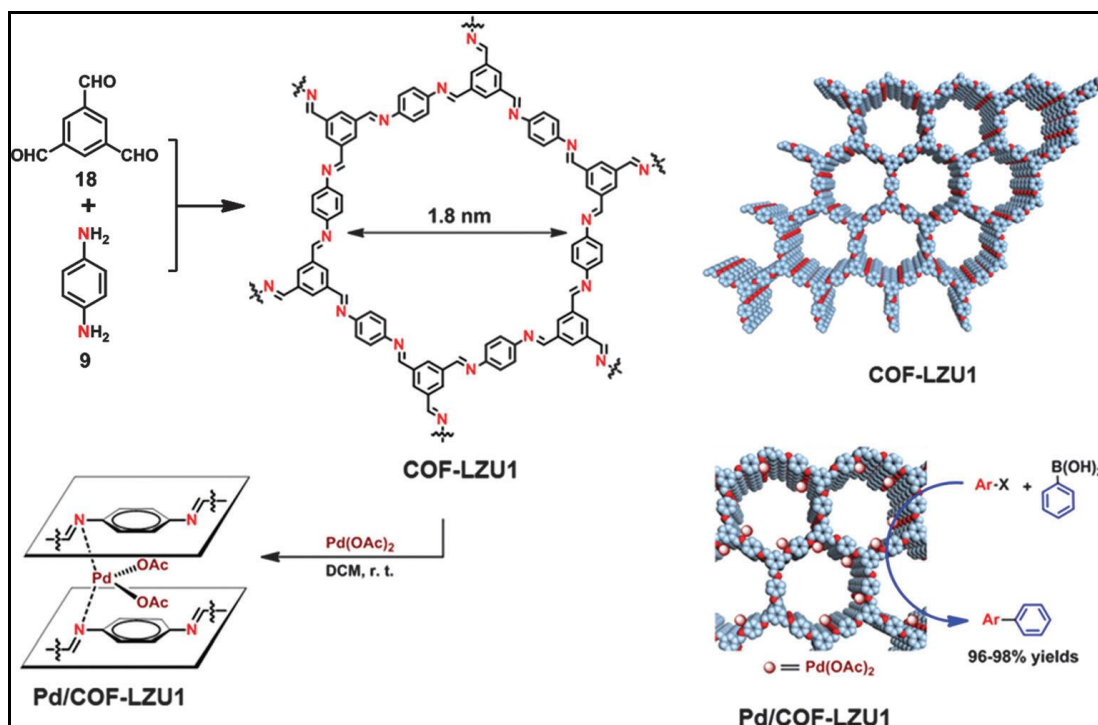
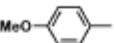
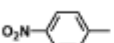
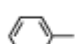
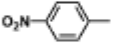
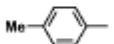
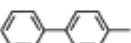

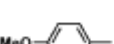


Figure 11: Chemical and extended structures of COF-LZU1 and Pd/COF-LZU1.²² (Reprinted with permission from Ref. 22. Copyright 2014 J. Am. Chem. Soc.).

Intrigued by using the Schiff-base metal complex as the homogeneous catalysts, they synthesized a new imine-linked COF material (COF-LZU1) from simple building units 18 and 9. The 2D eclipsed layered-sheet structure of COF-LZU1 renders the distance of nitrogen atoms to be 3.7 Å in the adjacent layers, which is suitable for the

strong coordination of metal ions. Accordingly, they synthesized the Pd(II)-coordinated COF-LZU1 via a simple treatment with Pd(OAc)₂ at room temperature. The structural preservation and robust Pd(II)-incorporation in the obtained Pd/COF-LZU1 were further verified by the PXRD, solid-state NMR, and XPS analyses. Pd/COF-LZU1 was then tested for catalyzing the Suzuki-Miyaura coupling reaction.²² The excellent catalytic performance was elucidated by the broad scope of the reactants, the excellent yields (96-98%) of the reaction products, with the high stability and easy recyclability of the catalyst. Catalytic activity of Pd/COF-LZU1 in the Suzuki–Miyaura coupling reaction (Table 2).

Table 2 : Catalytic activity of Pd/COF-LZU1 in the Suzuki–Miyaura coupling reaction.²²
(Reprinted with permission from Ref. 22. Copyright 2014 J. Am .Chem. Soc.).

$\text{R-X} + \text{C}_6\text{H}_5\text{-B(OH)}_2 \xrightarrow[\text{K}_2\text{CO}_3, \text{p-xylene}]{0.5 \text{ mol\% Pd/COF-LZU1}} \text{R-C}_6\text{H}_5$				
Entry ^a	R	X	Time (h)	Yield ^b (%)
1		I	3	96
2		I	2	97
3		Br	3	97
4		Br	3	97
5		Br	3	97
6		Br	2.5	98
7		Br	2.5	97
8		Br	4	96

^a Reaction conditions: aryl halide (1.0 mmol), phenylboronic acid (1.5 mmol), K₂CO₃ (2.0 mmol), and Pd/COF-LZU1 (0.5 mol%), 4 mL of *p*-xylene, 150 °C. ^b Isolated yield.

Chapter 2. Porphyrin based COFs:

2.1. Introduction:

Porphyrins are another interesting type of large, planar macrocyclic compounds with 18-electron systems and therefore, have been applied in the synthesis of porous materials. Recent research indicates that porphyrins are also suitable building units for constructing functional COFs.

2.2 Applications of porphyrin based COFs:

Recently Jiang and co-workers started working and they constructed the first porphyrin-based COF (ZnP-COF) via the boronate esterification reaction of zinc(II) 5,10,15,20-tetrakis(4-(dihydroxyboryl)phenyl) porphyrin 30b and 1,2,4,5-tetra-hydroxybenzene 14a (Figure 12).²³ This ZnP-COF shows large surface area and some photoelectric properties, ZnP-COF is a tetragonal 2D eclipsed structure contain a large BET surface area of 1742 m² g⁻¹ and an average pore size of 2.5 nm. The photo-electronic properties have been studied for ZnP-COF and other two porphyrin based COFs (H2-COF and CuP-COF).²⁵ The eclipsed alignment of these COF materials provides the possibility of carrier transportation within the porphyrin. H2-COF exhibits a hole transport with metal free porphyrin macrocycles. Due to the formation of metal-on-metal channels in the metal-porphyrin macrocycles with different electron densities, ZnP-COF and CuP-COF show high-rate ambipolar and electron conduction, respectively. Yaghi and co-workers have been synthesized Another two 2D non-metal porphyrin COF materials (COF-366 and COF-66) which shows high charge carrier mobility.²⁴ COF-366 was obtained via the formation of imine bonds between tetra(p-amino-phenyl)porphyrin³¹ and terephthaldehyde.⁶ COF-66 was synthesized via the boronic esterification reaction of tetra(p-boronic acid-phenyl)porphyrin^{30a} and 2,3,4,5-tetrahydroxy anthracene.^{15a} Both COF-366 and COF-66 show the hole conducting with high motilities.

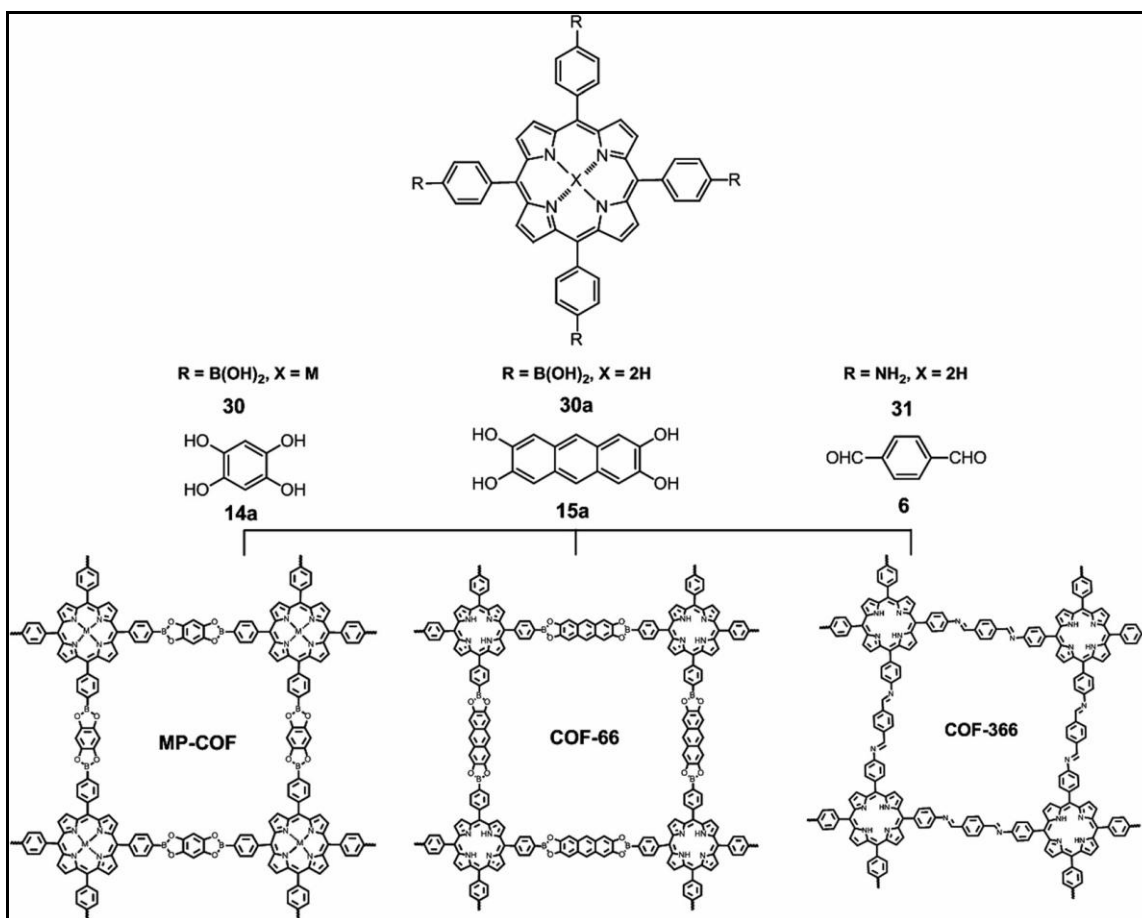


Figure 12: Building units and chemical structures of porphyrin-based COFs.^{23,24,25} (Reprinted with permission from Ref. 25. Copyright 2014 Angew. Chem. Int. Ed.).

2.3. Problem in Porphyrin based COFs:

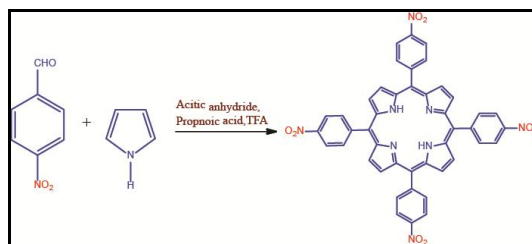
These are the main problems in porphyrin based COFs:

1. Crystallinity
2. Chemical Stability
3. Less surface area and porosity

In order to solve the above mentioned issues related to COFs, concept like keto-enol tautomerism as well as H-bonding has been applied.

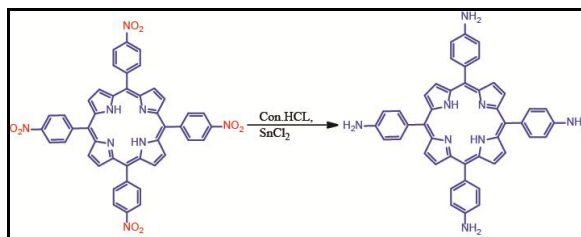
2.4 Synthesis of DhaTph containing intramolecular H-Bonding.

2.4.1.1 Synthesis of 5,10,15,20-Tetrakis(4-aminophenyl)-21H,23H-porphine (Tph):



Scheme 2: Synthesis of 5,10,15,20-Tetra(nitro)phenyl-21H,23H-porphyrin

Under air, a solution of 4-nitrobenzaldehyde (8.0 g, 5.2×10^{-2} mol) and acetic anhydride (4 mL) in propionic acid (200 mL) was heated at 100°C. Pyrole (3.9 mL, 2.6×10^{-2} mol) was added drop wise to the hot solution and the mixture was maintained at 100°C for a further hour. The resulting solution was allowed to cool and stand in air for 18 h. Filtration of the tar-like mixture afforded a black solid which was washed with water (5×100 mL) and dried in vacuo. The residue was taken into pyridine (100 mL) and heated to 120 °C for 1 h. The resulting mixture was hot filtered to remove any residual solid and the pyridine removed under vacuum. Soxhlet extraction of the black solid with acetone afforded a purple solid (1.95 g, 18 %). ^1H NMR ($\text{CDCl}_3/\text{DMSO-d}_6$): δ 0.02 (s, 2H,), 8.59 (s, 8H), 8.84 (d, $J = 9.0$ Hz, 8H), 8.87 (d, $J = 9$ Hz, 8H).

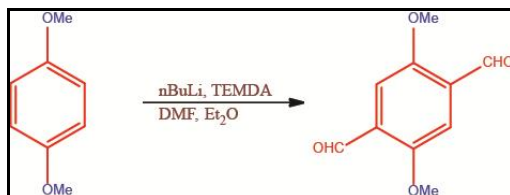


Scheme 3: Synthesis of 5,10,15,20-Tetrakis(4-aminophenyl)-21H,23H-porphine (Tph).

The 5,10,15,20-tetrakis(4-nitrophenyl)-21H,23H porphyrin (1.04 g, 1.29×10^{-3} mol) was dissolved in hot HCl (125 mL) at 70°C, to which was added $\text{SnCl}_2 \cdot 2\text{H}_2\text{O}$ (4.5 g, 1.99×10^{-2} mol). The resulting mixture was stirred at 70°C for 30 min and then cooled to 0°C. After neutralization with aqueous NH_3 , the resulting gray crystalline product was collected by filtration and dissolved in acetone. Rotary evaporation of the solution

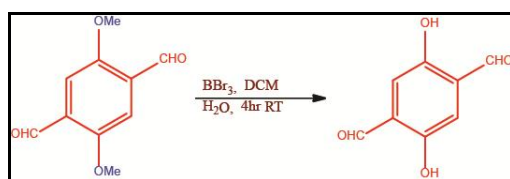
followed by drying under vacuum yielded as a purple color compound (0.92 g, 92 %). ^1H NMR (CDCl_3 , 300 MHz, ppm): δ -2.7 (s, 2H), 4.0 (s, 8H), 7.1-8.0 (m, 16H), 8.9 (s, 8H).

2.4.2.2. Synthesis of 2,5-Dihydroxy-1,4-benzenedicarboxaldehyde :



Scheme 4: synthesis of 2,5-Dimethoxy-1,4-benzenedicarboxaldehyde.

Add TMEDA (5 eq., 10.36 mL, 90.0 mmol) in a solution of 1,4-dimethoxybenzene (2.48 g, 18.0 mmol) and diethyl ether (60.0 mL) in a two neck round bottom flask. The mixture was cooled in an ice bath ($0\text{ }^\circ\text{C}$). After that n -Butyl lithium 2.5 M in hexane (36.2 mL, 90.0 mmol) was added drop wise slowly over 1–2 min. The reaction mixture was heated with at $50\text{ }^\circ\text{C}$ for further reflux for 10 h. During the time a light yellow precipitate was formed which was assumed to be the intermediate lithium salts. After that the DMF (7.0 mL, 90 mmol) was added to the mixture at the end of the metalation, and keep the reaction for 30 min. The reaction was quenched by 100 ml water and 20 ml of 3N HCl. The mixture was extracted with ether (3x100 mL). The Combined organic layers were separated and dried over anhydrous Na_2SO_4 . Solvent was evaporated under reduced pressure and the crude product was purified by column Chromatography (ethyl acetate / hexane, 1: 9) to afford pure compound (1.64 g, 55 %). The spectral data ^1H NMR (300 MHz, CDCl_3): δ = 10.50 (s, 2H), 7.45 (s, 2H), 3.94 (s, 6H); ^{13}C NMR (75 MHz, CDCl_3): δ = 189.2, 155.7, 129.1, 110.9, 56.2.

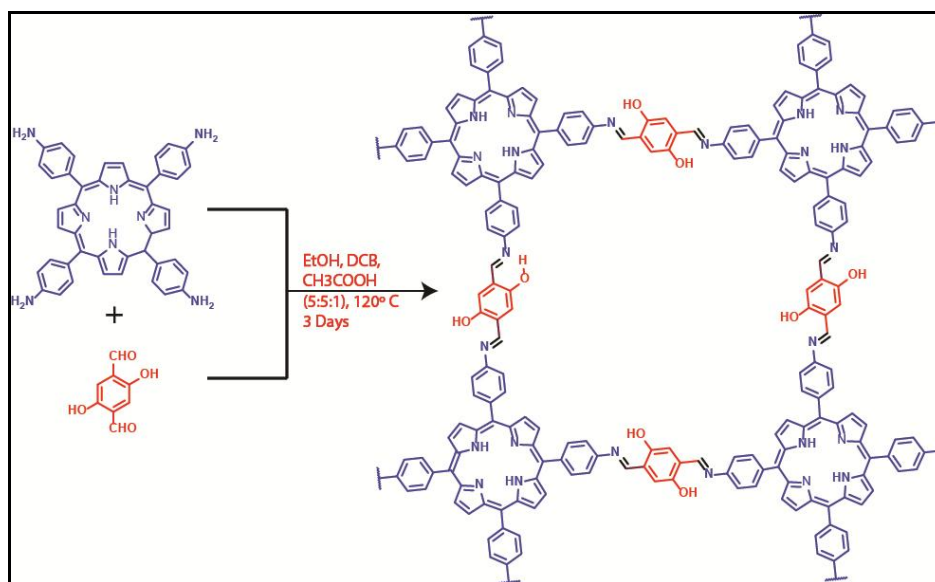


Scheme 5: Synthesis of 2,5-dihydroxy-1,4-benzenedicarboxaldehyde.

To a solution of 2,5-Dimethoxy-1,4-benzenedicarboxaldehyde (1.59 g, 8.19 mmol) in dichloromethane (70 mL) cooled at $0\text{ }^\circ\text{C}$. Then boron tribromide (31.0 mL,

31.0 mmol; 1 M solution in hexane) was added dropwise over 20 min. The mixture was stirred for 4h at room temperature and checked the TLC. After completion of reaction adds water (70 mL) and stirred for 30 min. The reaction was quenched by 20 ml water, and the mixture was extracted with DCM (3x30 mL). The Combined organic layers were separated and dried over anhydrous Na₂SO₄. Solvent was evaporated under reduced pressure and the crude product was purified by column Chromatography (ethyl acetate / hexane, 3: 7) to afford pure compound (1.29 g, 95 %). The spectral data ¹H NMR (300 MHz, CDCl₃): = 10.74 (s, 2H), 10.42 (s, 2H), 7.36 (s, 2H); ¹³C NMR (75 MHz, CDCl₃): δ = 191.8, 153.8, 128.2, 116.6.

2.4.3.1. Synthesis of DhaTph:



Scheme 6: Synthesis of **DhaTph**.

The synthesis of **DhaTph**²⁹ was carried out by using solvothermal synthesis method. The 2,5-dihydroxyterephthalaldehyde (**Dha**) (26.6 mg, 0.16 mmol) and tetra(p-amino-phenyl)porphyrin (**Tph**) (54.0 mg, 0.08 mmol) was mixed in presence of 6.0 M acetic acid (0.4 mL) using solvent 1,2-dichlorobenzene, ethanol (1:1) as solvent combination (4 mL). This mixture was sonicated for 10-15 minutes. The tube was then frozen at 77 K (liquid N₂ bath) and degassed by 3-4 times at maintain proper interval time. After finishing cycles, the tube was sealed and then heated at 120 °C for 72 h.

After 72 h, the reaction stopped slowly cool down. The COF material washed with ethanol and dried under vacuum at 150 °C for 10 hours to give purple colored powder in 79 % (56 mg) isolated yield based on Tph.

2.2.5. Characterization of DhaTph

2.2.5.1 FT-IR of DhaTph

In the FT-IR spectrum of COFs, stretching frequency of amino group (3100-3400 cm^{-1}) in **Tph** the carbonyl group (1665 cm^{-1}) in **Dha** was disappeared (**Figure 13**), which be a sign of the total consumption of reactants. The formation of product imine bond can be understood from the FT-IR spectrum of **DhaTph** since it shows the representative imine -C=N stretching frequency at 1612 cm^{-1} , which is coming close to the COF-366 (1620 cm^{-1}).⁹

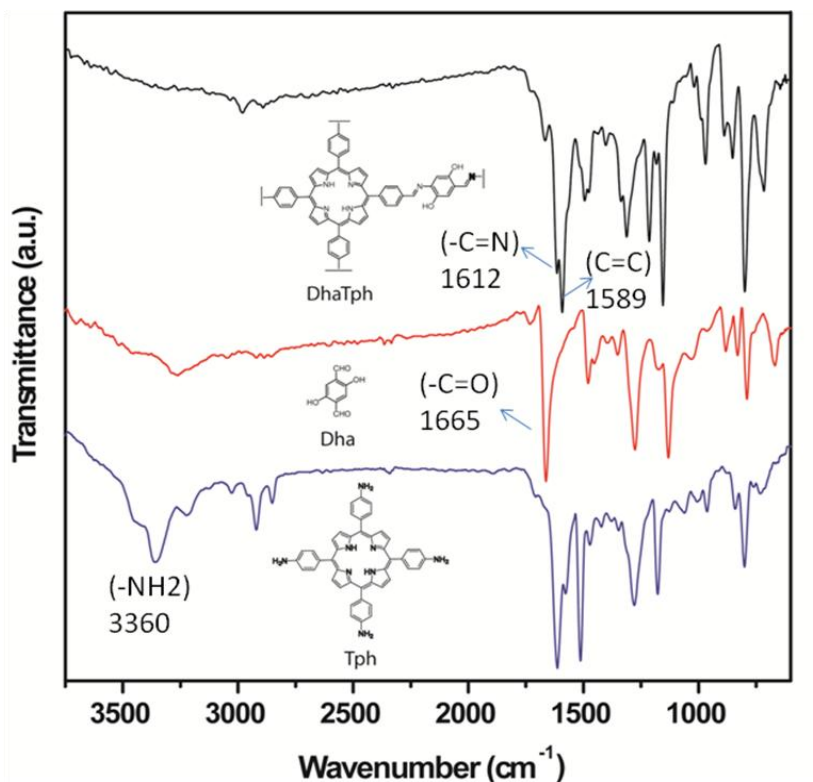


Figure 13: FT-IR spectra of **DhaTph** (black), (**Dha**) (red), and (**Tph**) (blue).

2.2.5.2 PXRD Pattern of DhaTph:

The PXRD pattern of DhaTph showed good quality crystallinity, with a high intense diffraction peak at 3.4° which corresponds to (100) plane reflections of the COF together with low intensity diffraction peak at 6.9° and $20\text{-}23^\circ$ 2θ which were assigned for (200) and (001) facets. The presence of broad peak at $20\text{-}23^\circ$ in DhaTph diffraction pattern was attributed to the defects in the $\pi\text{-}\pi$ stacking between the successive COF layers. The reason behind this high crystallinity is that, **DhaTph** possess strong intramolecular hydrogen bonding in $\text{O}\text{-H}\dots\text{N}=\text{C}$ bonds which helpful to holds all phenyl rings in one plane and remains all imine bonds $\text{-C}=\text{N}$ in the trans conformation. These phenomena help to minimize the structural defects as well as build-up the structural rigidity resulting in enhanced crystallinity of material.

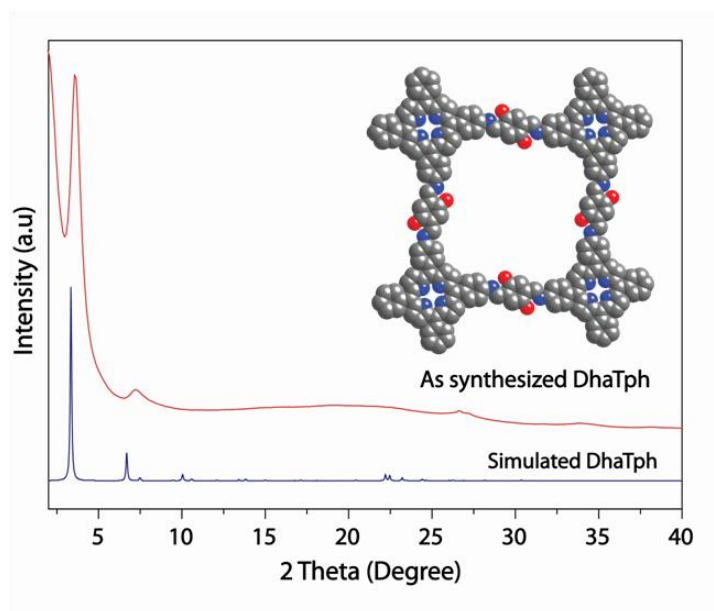


Figure14: PXRD pattern of **DhaTph** (red), Simulated (blue).

2.2.5.3 Solid state ^{13}C -NMR:

The formation of **DhaTph** was confirmed by solid state ^{13}C CP-MAS NMR spectrum. The spectral data of **DhaTph** confirms the formation of imine $\text{-C}=\text{N}$ bond, as it shows the characteristic signal at δ 161.8 and along with the other required carbon signal like δ 153.1, 148.3, 140.7, 137.1, 132.5, 120.7 confirmed the COF material.

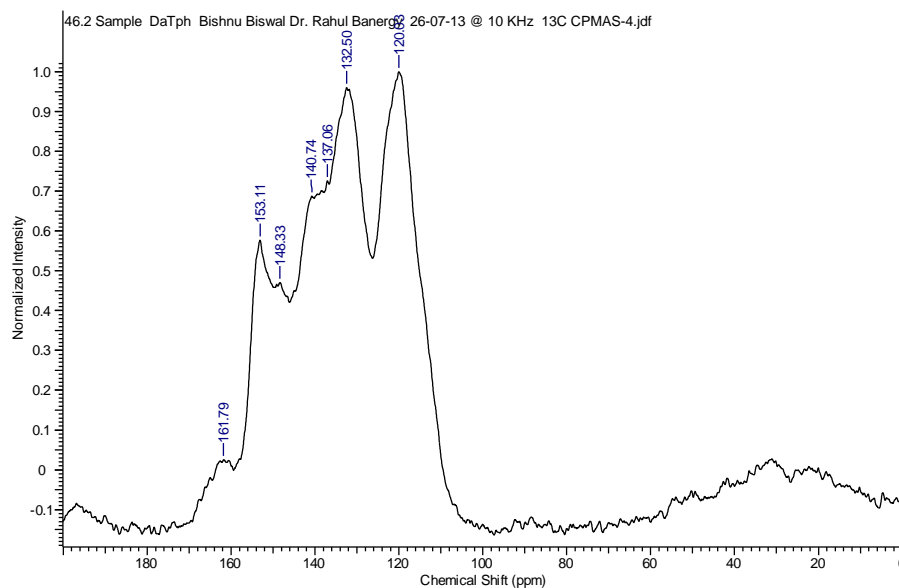


Figure 15: ^{13}C CP-MAS NMR spectra of **DhaTph**.

2.2.5.4. Gas adsorption of **DhaTph**:

The N_2 adsorption isotherms were collected at 77 K for the activated COF to confirm the permanent porosity and structural rigidity. It showed a reversible type IV uptake isotherm and at low pressure (0-0.1 bar) sharp increase in N_2 uptake was obtained because of the filling of small pores and then gradual uptake with increasing up to 0.8 bar. The surface area of **DhaTph** ($1048 \text{ m}^2\text{g}^{-1}$) was calculated by applying Brunauer-Emmett-Teller (BET) model. The high surface area of **DhaTph** was due to the presence of strong intramolecular O–H...N=C hydrogen bonding present in the *trans* confirmation of imine bond ($-\text{C}=\text{N}$). It helps to improve the planarity of the system and minimizes the defects in structure as a result improved crystallinity and surface area was observed for **DhaTph**. The pore width of **DhaTph** was calculated to be 20.1 \AA for by using NLDFIT method, which is in close agreement with the theoretically predicted pore width of 20.1 \AA for **DhaTph**.

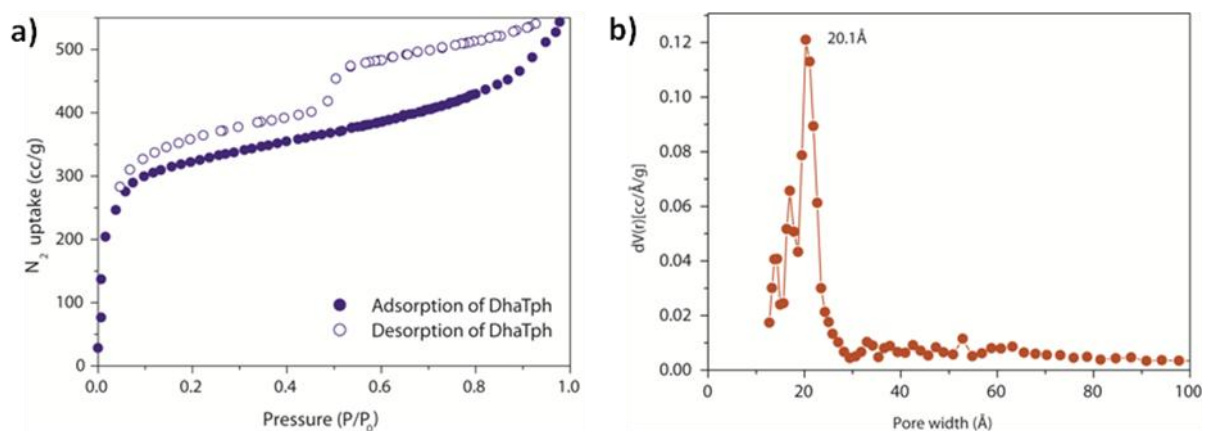


Figure 16: a) N_2 adsorption and desorption Isotherm of **DhaTph**, b) pore size distribution of **DhaTph**.

2.2.5.5. SEM and TEM of DhaTph:

The morphologies of **DhaTph** were investigated by employing SEM and TEM. The SEM analyses of **DhaTph** (**Figure17 a**) show the agglomeration of particles forming globular morphologies. The TEM images of the **DhaTph** (**Figure17 b**) are like rectangle shaped with particle size near to ~ 60 nm.

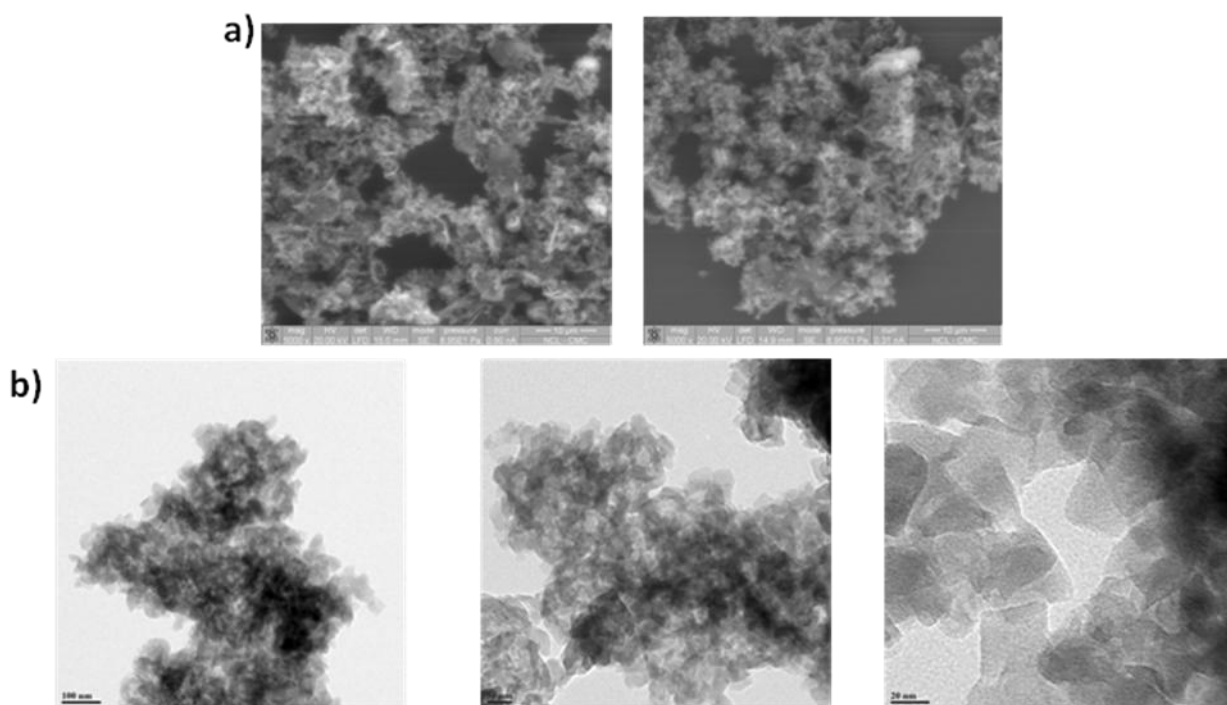


Figure 17: a) SEM and b)TEM morphologies **DhaTph**.

2.2.5.6 TGA of DhaTph:

Thermo gravimetric analysis (TGA) were carried out on a TGA 50 analyzer (Mettler-Toledo) or a SDT Q600 TG-DTA analyzer under N₂ atmosphere at a heating rate of 10 °C min⁻¹ within a temperature range of 30-900 °C. The thermal stability of activated COF was confirmed by TGA analysis. This COF showed high thermal stability up to 300°C and there were no guest molecules inside the pores). The decomposition of the frameworks were observed after 300°C with gradually weight loss of 30% for **DhaTph** (Figure 18).

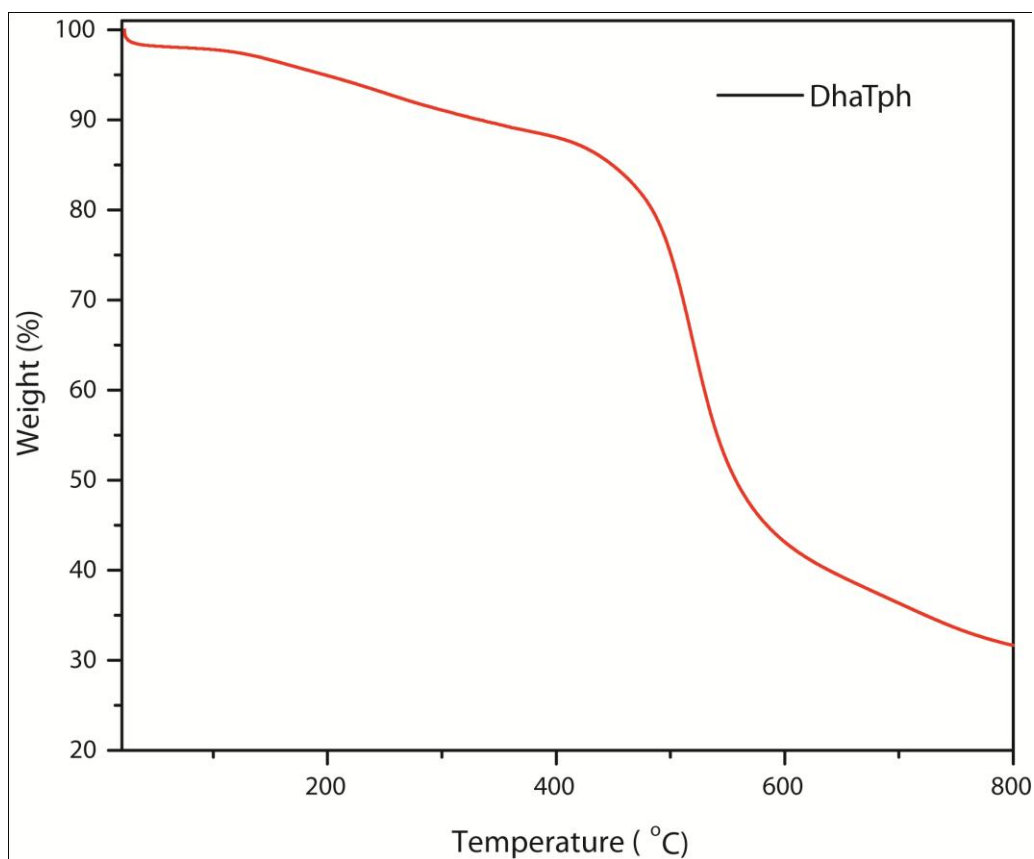


Figure 18: TGA analysis of **DhaTph**.

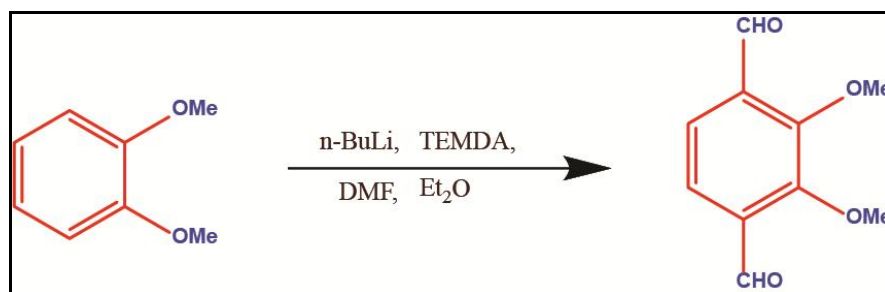
Chapter 3. New Porphyrin based COFs Containing Intramolecular H-Bonding for the Enhancement of its Stability and Crystallinity

3.1. Introduction:

Since 2D porphyrin containing COFs have been reported to show high rate charge carrier conduction and photoconductivity due to the long range π -orbital overlapping of porphyrin units.,^{24,25,26} Now, in order to enhance the chemical stability and crystallinity in 2D porphyrin COFs, we have decided to switch to a new strategy to protect the COF interior by introducing –OH functionalities adjacent to the Schiff base [–C=N] centers in COFs and thereby creating an intramolecular O–H...N=C hydrogen bonding.

3.2 Present Work:

3.2.1 Synthesis of 2,3-dihydroxy-1,4-benzenedicarboxaldehyde²⁸:

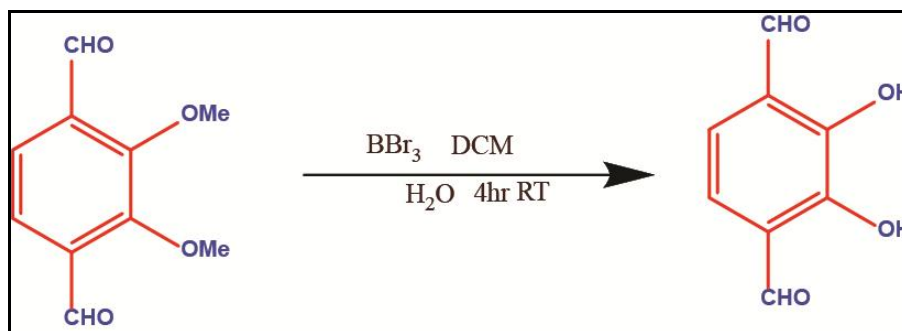


Scheme 7: synthesis of 2,3-Dimethoxy-1,4-benzenedicarboxaldehyde

Add TMEDA (5 eq., 10.36 mL, 90.0 mmol) in a solution of 1,2-dimethoxybenzene (2.48 g, 18.0 mmol) and diethyl ether (60.0 mL) in a two neck round bottom flask. The mixture was cooled in an ice bath (0 °C). After that *n*-Butyl lithium 2.5 M in hexane (36.2 mL, 90.0 mmol) was added drop wise slowly over 1–2 min. The reaction mixture was heated with at 50 °C for further reflux for 10 h. During the time a light yellow precipitate was formed which was assumed to be the intermediate lithium salts. After that the DMF (7.0 mL, 90 mmol) was added to the mixture at the end of the metalation, and keep the reaction for 30 min. The reaction was quenched by 100 ml water and 20 ml of 3N HCl. The mixture was extracted with ether (3x100 mL). The Combined organic layers were separated and dried over anhydrous Na₂SO₄. Solvent was evaporated under reduced pressure and the crude product was purified by column Chromatography (ethyl acetate /

hexane, 1: 9) to afford pure compound (1.69 g, 57 %). The spectral data ^1H NMR (300 MHz, CDCl_3): δ 10.44 (2H, s), 7.63 (2H, s), 4.05 (6H, s); ^{13}C NMR (75 MHz, CDCl_3): δ 189.5, 156.9, 134.4, 123.1, and 62.9.

3.2.3.2. Synthesis of 2,3-dihydroxy-1,4-benzenedicarboxaldehyde:



Scheme 8: synthesis of 2,5-dihydroxy-1,4-benzenedicarboxaldehyde.

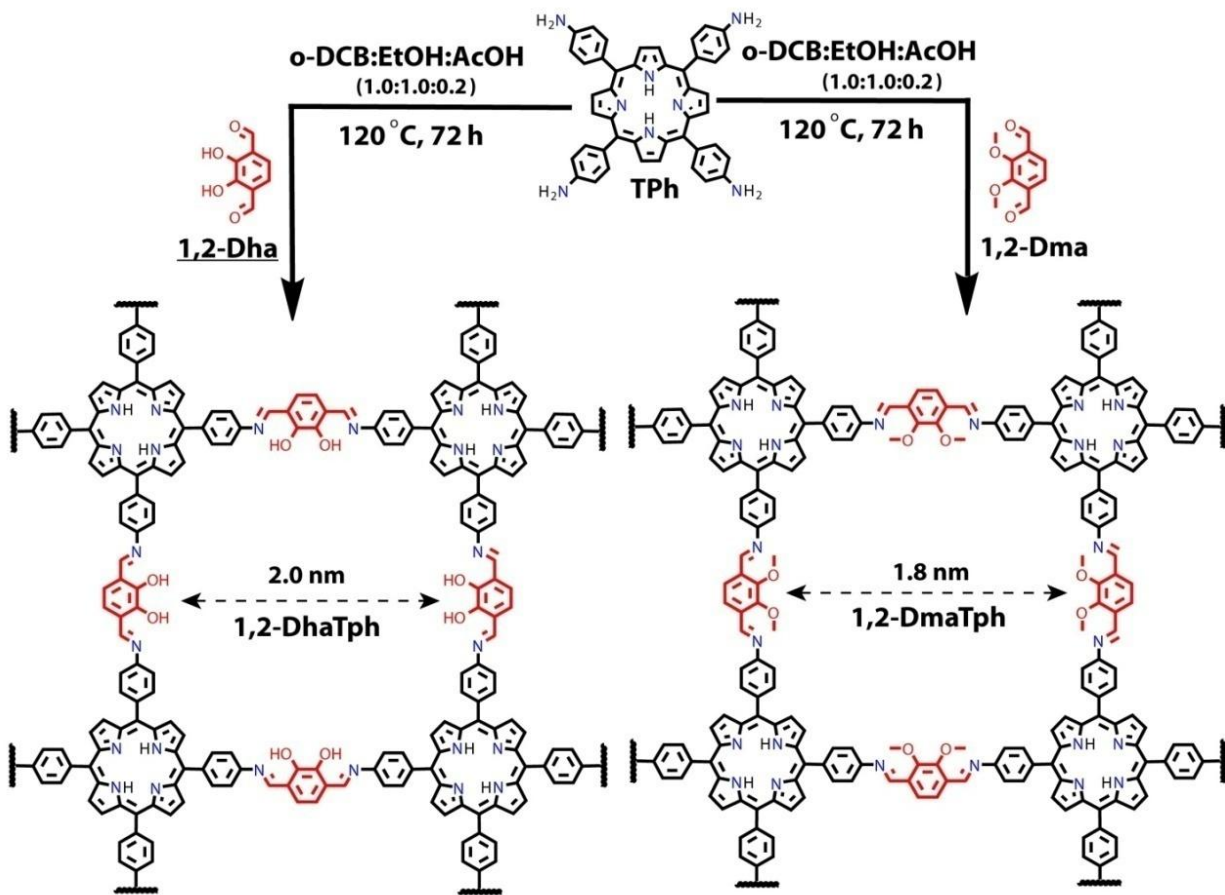
To a solution of 2,3-Dimethoxy-1,4-benzenedicarboxaldehyde (1.59 g, 8.19 mmol) in dichloromethane (70 mL) cooled at 0°C . Then boron tribromide (31.0 mL, 31.0 mmol; 1 M solution in hexane) was added drop wise over 20 min. The mixture was stirred for 4h at room temperature and checked the TLC. After completion of reaction adds water (70 mL) and stirred for 30 min. The reaction was quenched by 20 ml water, and the mixture was extracted with DCM (3x30 mL). The Combined organic layers were separated and dried over anhydrous Na_2SO_4 . Solvent was evaporated under reduced pressure and the crude product was purified by column Chromatography (ethyl acetate / hexane, 3: 7) to afford pure compound (1.30 g, 96 %). The spectral data ^1H NMR (300, MHz, CDCl_3): δ 7.28 (s, 2H), 10.03 (s, 2H), 10.91 (s, 2H); ^{13}C NMR (75, MHz, CDCl_3): δ 122.1, 123.0, 150.8, and 196.2

3.2.4. Synthesis of 1,2-DhaTph and 1,2-DmaTph:

We have synthesis of **1,2-DhaTph** and **1,2-DmaTph** COFs by applying same concept of strong intramolecular hydrogen bonding. These COFs were synthesized by the reaction between 1,2-dihydroxyaldehyde or 1,2-methoxyaldehyde and 5,10,15,20-tetrakis(4-aminophenyl)-21H,23H-porphine unit. In the case of **1,2-DhaTph** showed more surface area in comparison with that of **1,2-DmaTph** due to intramolecular H-

bonding and also maintains the planarity of structure. In the case of **1,2-DmaTph** showed less surface area due to the no intramolecular H-bonding and loss of planarity. In this chapter we will comparative study of **1,2-DhaTph** and **1,2-DmaTph** of porosity, crystallinity, chemical and thermal stability of materials.

3.2.4.1. Synthesis of 1,2-DhaTph and 1,2-DmaTph:



Scheme 9: Synthesis of **1,2-DhaTph** and **1,2-DmaTph**.

The COFs, **1,2-DhaTph** and **1,2-DmaTph** were synthesized by reversible Schiff-base reaction using 5,10,15,20-tetrakis(4-aminophenyl)-21H,23H-porphine unit (**Tph**) (56.0 mg, 0.08 mmol) and 1,2-dihydroxyterephthalaldehyde (**1,2-Dha**) (26.6 mg, 0.16 mmol) or 1,2-methoxyterephthalaldehyde (**Dma**) (31.0 mg, 0.16 mmol) in dichlorobenzene (o-DCB) and ethanol (EtOH) (1:1 mL) solvent combination with catalytic amount of 6.0 M acetic acid (0.2 mL) (**Scheme 9**).

In the FT-IR spectrum of **1,2-DhaTph** and **1,2-DmaTph** COFs, stretching frequency of amino group ($3100-3400\text{ cm}^{-1}$) in **Tph**, carbonyl group (1660 cm^{-1}) in **1,2-Dha** and **1,2-Dma** (1671 cm^{-1}) were disappeared, which be a sign of the total consumption of starting materials. The formation of imine bond can be understood from the FT-IR spectrum of **1,2-DhaTph** and **1,2-DmaTph** since it shows the characteristic imine -C=N stretching frequency at 1609 cm^{-1} and 1613 cm^{-1} respectively, which is coming close to the **DhaTph** (1613 cm^{-1}) and COF-366 (1620 cm^{-1}).⁹

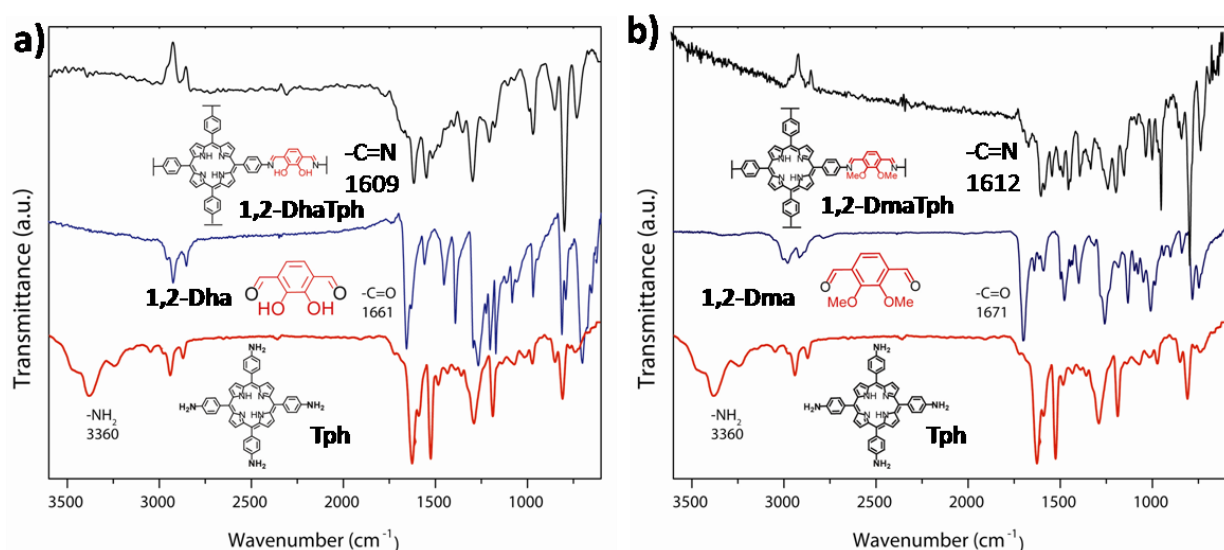


Figure 19: a) FT-IR spectra of **1,2-DhaTph** (black), (**Dha**) (blue), and (**Tph**) (Red).linker unit (blue); b) FT-IR spectra of **1,2-DmaTph** (black), (**Dma**) (blue), and (**Tph**) (Red).linker unit (blue).

3.2.4.2. PXRD Pattern of 1,2- DhaTph and 1,2- DmaTph:

The PXRD pattern of **1,2-DhaTph** showed good crystallinity, with a high intense diffraction peak at 3.3° which corresponds to (100) plane reflections of the COF together with low intensity diffraction peak at 7.0° and $18-22^\circ$ 2θ which were assigned for (200) and (001) facets. The presence of broad peak at $18-22^\circ$ in **1,2-DhaTph** diffraction pattern was attributed to the defects in the π - π stacking between the successive COF layers. It was observed that in **1,2-DhaTph** the peak intensity of the 100 plane become more as compared to that of **1,2-DmaTph** (approximately 7000 cps). PXRD peaks for **1,2-DmaTph** were looked nearly at the same peak position to that of **1,2-DhaTph**. The **1,2-DmaTph** showed moderate crystallinity because Peaks at 3.3° , 7.0° , $15-27^\circ$ correspond to 100, 200, 001 facets respectively. But the peak intensity of the 100 plane

has been considerably reduced compared to **1,2-DhaTph** (**Figure 20**). In the case **1,2-DhaTph** has strong intramolecular Hydrogen bonding that helps to minimize the structure defects as result maintain the planarity of framework. But in the case of **1,2-DmaTph** has no intramolecular Hydrogen bonding also loss of planarity. From this analysis, we conclude that the **1,2-DhaTph** showed more crystalline than **1,2-DmaTph**.

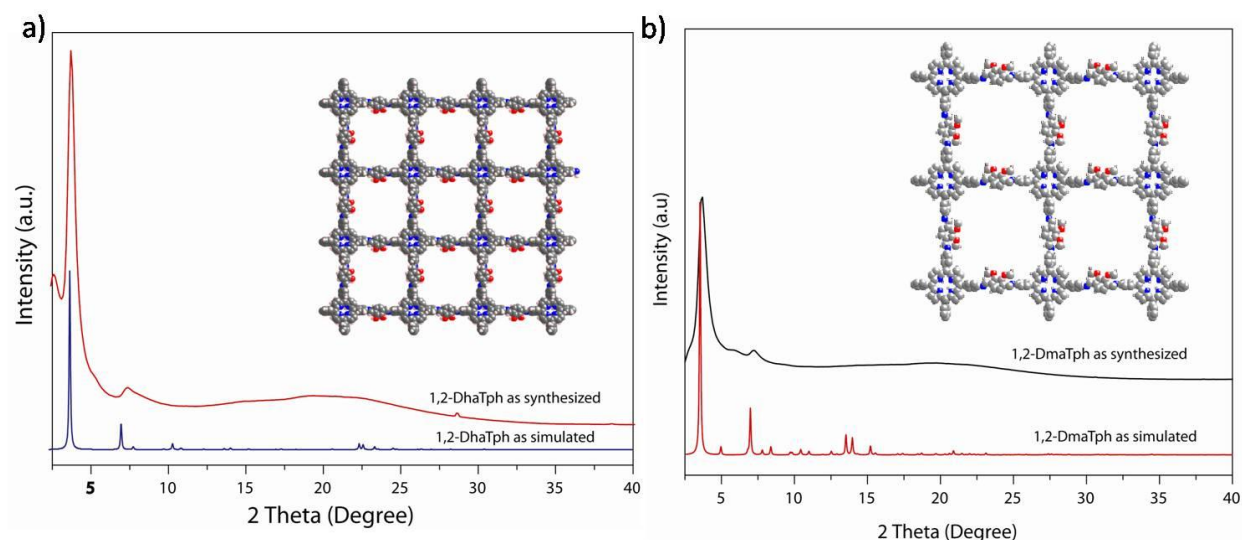


Figure 20: a) PXRD pattern of **1,2-DhaTph** (red), Simulated (blue). b) PXRD pattern of **1,2-DmaTph** (black), Simulated (red).

3.2.5.3 Solid state ^{13}C -NMR:

The solid state ^{13}C CP-MAS NMR spectrum of **1,2-DhaTph** and **1,2-DmaTph** confirms the formation of imine $-\text{C}=\text{N}$ bond, as it shows the characteristics signals at δ 159.8 and 154.4 respectively (**Figure 21**). These chemical shifts of imine $-\text{C}=\text{N}$ which is coming close to the COF-366 (δ 158.5).⁹ and **1,4-DhaTph** (δ 161.8).

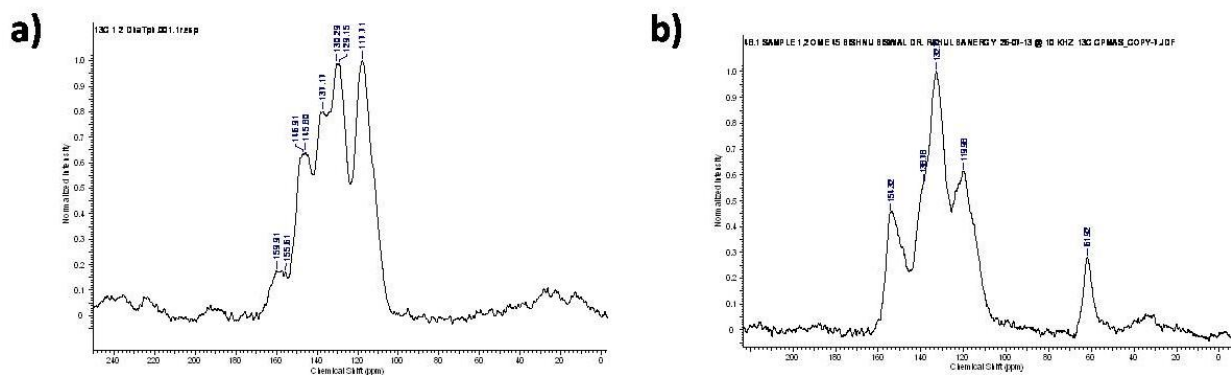


Figure 21: (a) ¹³C CP-MASNMR spectra of **1,2-DhaTph**; (b) ¹³C CP-MAS NMR spectra of **1,2-DmaTph**.

3.2.5.4. Gas adsorption of **1,2-DhaTph** and **1,2-DmaTph**:

The N₂ adsorption isotherms were collected at 77 K for the activated COFs to confirm the permanent porosity and structural rigidity. It showed a reversible type IV uptake isotherm and at low pressure (0-0.1 bar) sharp increase in N₂ uptake was obtained because of the filling of small pores and then gradual uptake with increasing up to 0.8 bar. The N₂ uptakes observed at high relative pressure (P/P₀> 0.8 bar) was due to the condensation inside the interparticle voids. The surface area of **1,2-DhaTph** (612 m²g⁻¹) and **1,2-DmaTph** (428 m²g⁻¹) were calculated by applying Brunauer-Emmett-Teller (BET) model (**Figure 22**). The **1,2-DhaTph** was high surface area as compare to the **1,2-DmaTph**. The **1,2-DhaTph** have very strong intramolecular O–H...N=C hydrogen bonding present in the *cis* confirmation of imine bond (–C=N). This H-bonding interaction helps to improve the planarity of the system and minimizes the defects in structure as a result improved crystallinity and surface area were observed for **1,2-DhaTph**. However in **1,2-DmaTph** case no intramolecular H-bonding as result, its lose the planarity in structure, maximize the defects in structure showed less surface area.

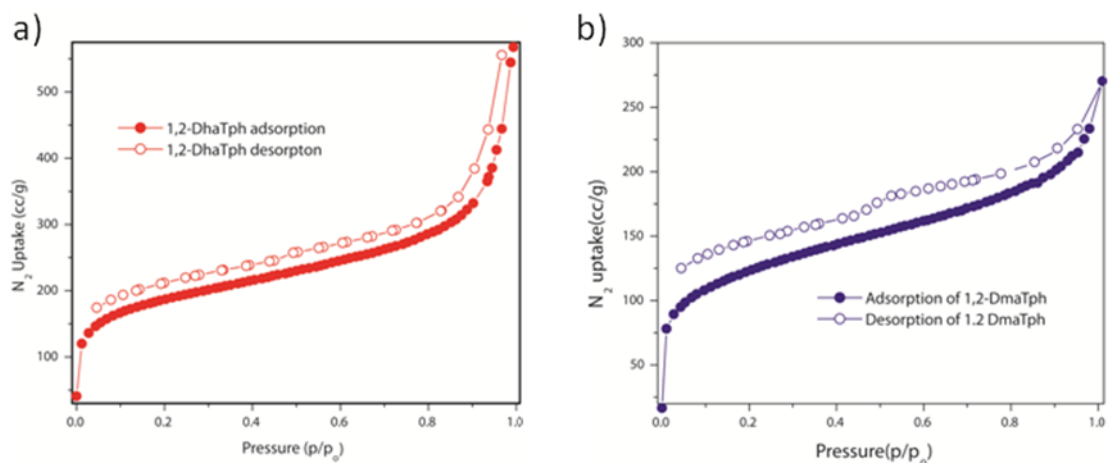


Figure 22: a) N_2 adsorption and desorption Isotherm of **1,2-DhaTph**; b) N_2 adsorption and desorption Isotherm of **1,2-DmaTph**.

3.2.5.5. SEM and TEM of 1,2-DhaTph and 1,2-DmaTph

The morphologies of these synthesized COFs were investigated by employing SEM and TEM (**Figure 23**). The SEM analyses of **1,2-DhaTph** show the agglomeration of particles forming globular morphologies. The TEM images of the **1,2-DhaTph** is composed of well defined, square shaped particles of size around 50 nm.

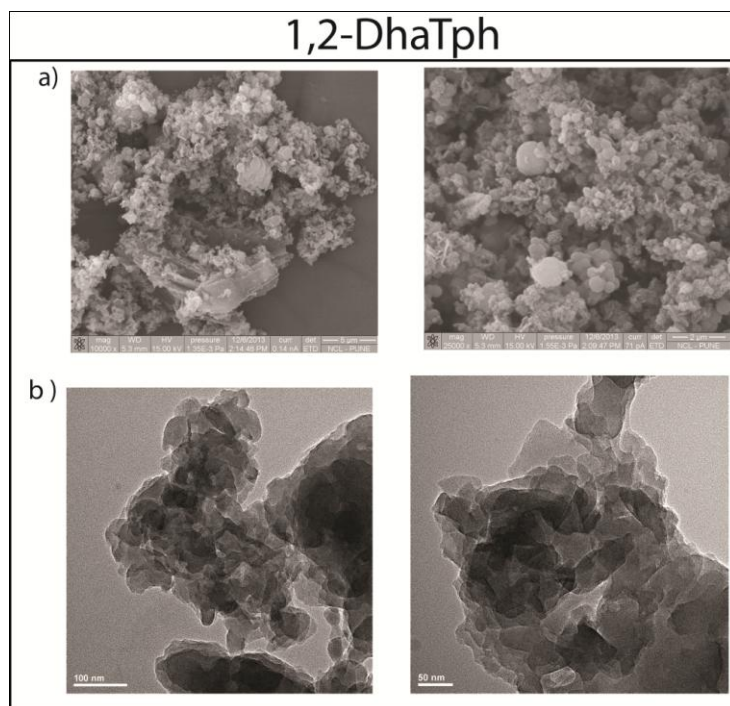


Figure 23: SEM and TEM morphologies **1,2-DhaTph**.

The morphologies of these synthesized COFs were investigated by employing SEM and TEM (**Figure 24**). The SEM analyses of **1,2-DmaTph** confirm the agglomeration of particles forming bulbous morphologies. The TEM images of the **1,2-DmaTph** is self-possessed of well defined, sheet shaped particles.

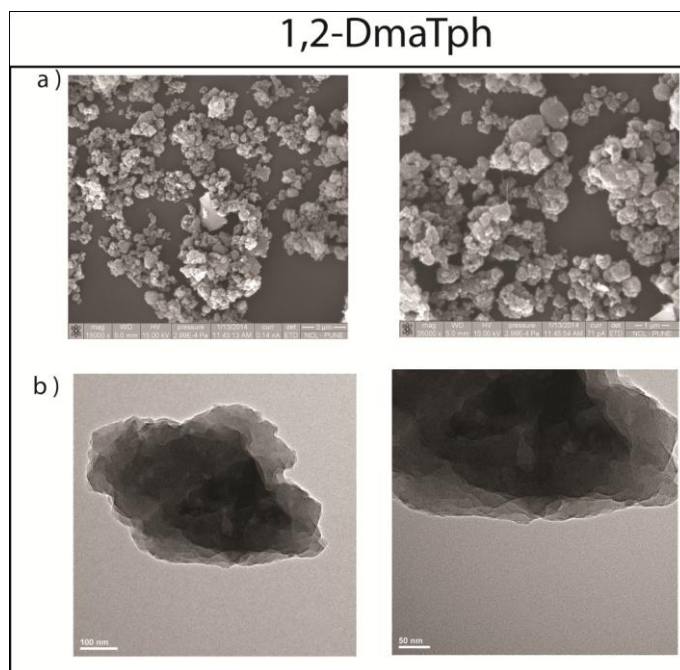


Figure 24: SEM and TEM morphologies **1,2-DmaTph**.

3.2.5.6 TGA of **1,2-DhaTph** and **1,2-DmaTph**

The thermal stability of activated **1,2-DhaTph** and **1,2-DmaTph COF** was confirmed by TGA analysis (**Figure 25**). The **1,2-DhaTph** showed high thermal stability up to 350 °C and there were no guest molecules inside the pores). **1,2-DmaTph** showed high thermal stability up to 300 °C and there were no guest molecules inside the pores). The decomposition of the frameworks were observed after 300 °C with gradual weight loss of 25 % for **1,2-DhaTph** and 20 % for **1,2-DmaTph**.

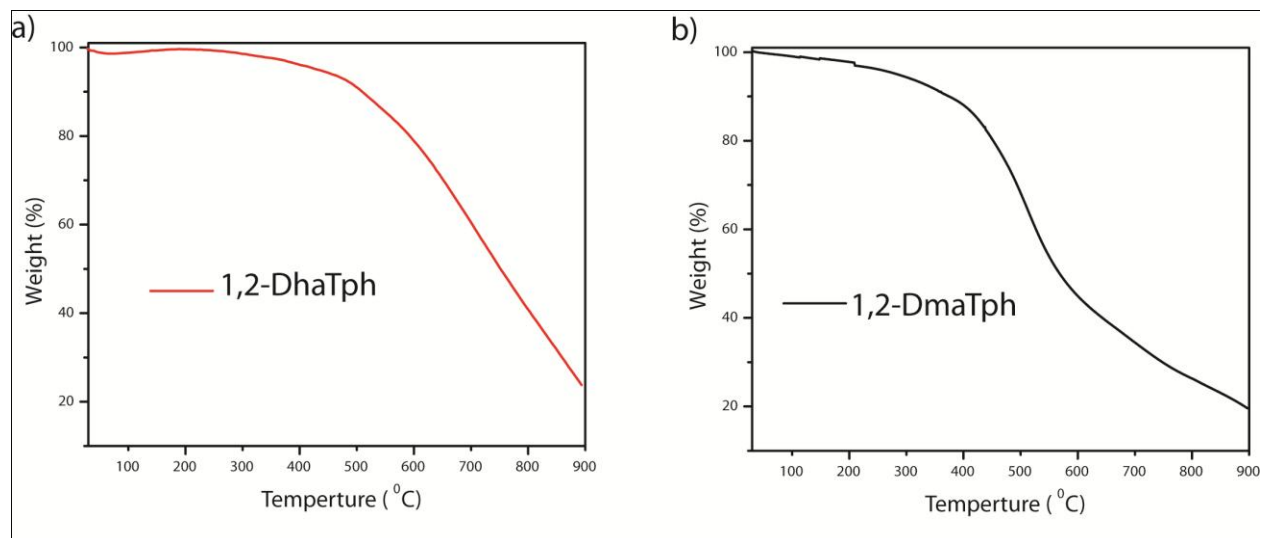


Figure 25: a) TGA analysis of **1,2-DhaTph**; b) TGA analysis of **1,2-DmaTph**.

3.2.6 Stability test of **1,2-DhaTph** and **1,2-DmaTph**:

The chemical stability test of COFs were test in aqueous, acidic (3N HCl) and alkaline (3N NaOH) medium. The **1,2-DhaTph** and **1,2-DmaTph** materials directly submerged in 10 mL water for more than 7 days. After this period, the materials were filtered, washed with water, ethanol, and dried it. The water treated materials were characterized by IR, PXRD and N₂ adsorption. The PXRD pattern of water treated COFs materials resemble with as synthesized COFs material. All the relative peaks intensity is matched to synthesized COFs materials. The surface area of water treated COFs has got very negligible difference in the surface area (before 611 m²g⁻¹ and after 485 m²g⁻¹ for **1,2-DhaTph**) and (before 428 m²g⁻¹ and after 374 m²g⁻¹ for **1,2-DmaTph**). These results show the remarkable hydrolytic stability of this COFs. The same procedure was followed for acid stability test. Initially green coloration was observed in the solution of both COFs. After this period, acid treated COF material were filtered, washed with water, ethanol and dried it. These COFs have some weight loss of near about 25-20% for **1,2-DhaTph** and 75-80 % for **1,2-DmaTph**. The acid treated materials were examined by PXRD, N₂ adsorption. The PXRD of **1,2-DhaTph** was data similar to as synthesized **1,2-DhaTph**. The surface area of acid treated COFs were observed that very significant changes like (before 611 m²g⁻¹ and after 318 m²g⁻¹ for **1,2-DhaTph**). These COFs showed excellent stability towards acid due to the protection of imine –

C=N by strong intramolecular hydrogen bonding. The PXRD of recovered sample (**1,2-DmaTph**) showed that nearly all the peaks are disappeared.

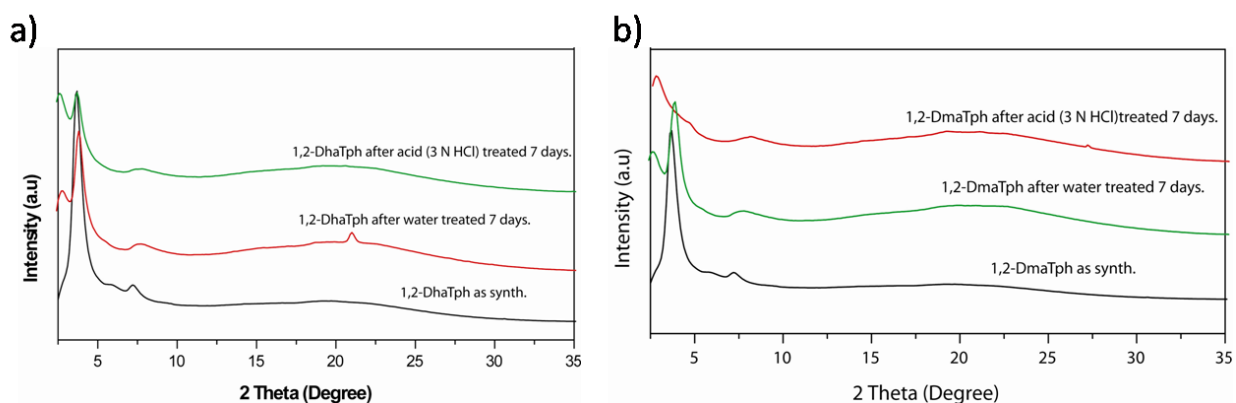


Figure 27: PXRD patterns of a) 1,2-DhaTph and b) 1,2-DmaTph for as synthesized water and acid treatment samples.

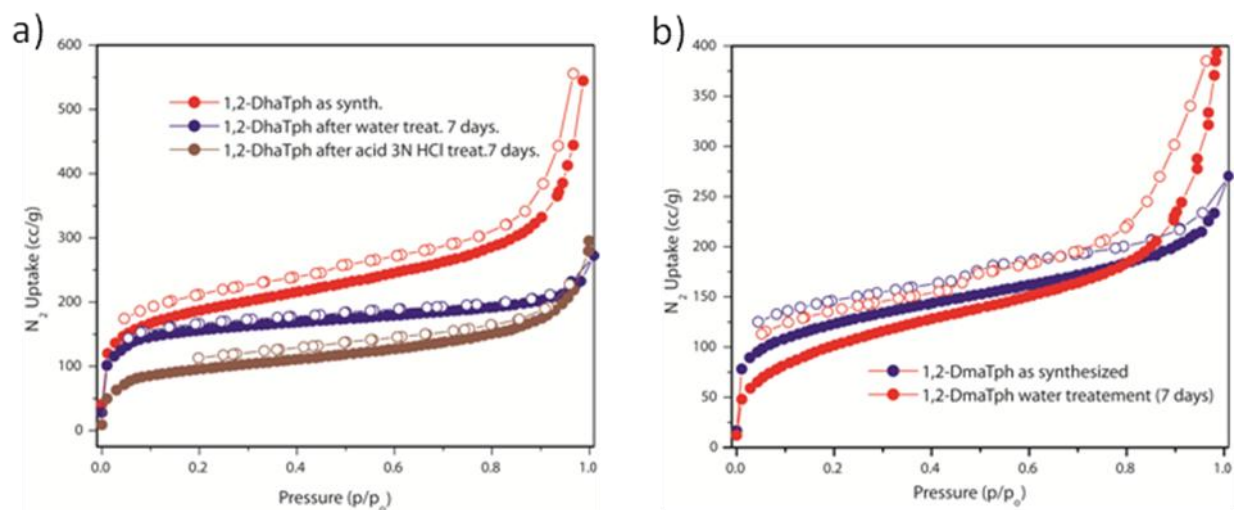


Figure 27: N₂ adsorption isotherms of a) 1,2-DhaTph and b) 1,2-DmaTph for as synthesized water and acid treatment samples.

Conclusion:

- 1) The Covalent Organic Frameworks (COFs) represent a fascinating new type of crystalline porous materials. The COF materials possess the advantages of low density, large surface area, tunable properties and functionality because of versatile covalent-bonding of organic building units consisting of light elements (C, Si, O, B and N) only. The regular pore structures have offered the COF materials with superior potentials in advanced applications.
- 2) In this work, extraordinary strategy of introduction of intramolecular O-H...N=C hydrogen bonding as a stabilizing factor, which helps to improve the crystallinity, porosity and chemical stability of the porphyrin containing covalent organic frameworks (COFs).
- 3) We have introduced -OH functionalities adjacent to the Schiff base [C=N] centers in a porphyrin containing COF (**1,2-DhaTph**) and thereby created an intramolecular O-H...N=C hydrogen bonding. Since the intramolecular O-H...N=C hydrogen bonding holds all phenyl rings in one plane and keeps imine bonds in trans form, crystallinity of **1,2-DhaTph** was greatly improved. This improved crystallinity was also reflected by the high surface area of the material. The most important observation we made was the enhancement of hydrolytic stability of **1,2-DhaTph** as a result of this strong intramolecular hydrogen bonding.
- 4) **1,2-DhaTph** retains its crystallinity for more than one week water and 3N hydrochloric acid. Our observation is highly important because similar porphyrin containing COFs reported in literature such as **COF-366** [*Chem. Mater.* **2011**, 23, 4094] and **CuP-Ph COF** [*J. Am. Chem. Soc.* **2013**, 135, 546] are not chemically stable and need anhydrous organic solvents for washing and purification.
- 5) In summary we could say that, we for the first time reported the utilization of the concept '*Intramolecular Hydrogen Bonding*' in COFs for the improvement of crystallinity, porosity and chemical stability.

Future plan:

1. Most studies to date have focused on the development of synthetic methodologies with the aim of maximizing pore size and surface area for gas storage. That means the functions of COFs have not yet been well explored. So my future plane is to synthesize different types of new functionalized COFs for increasing porosity and surface area for gas storage.
2. Synthesis of Metal doping porphyrin based COFs, for the semi-conductive and photoconductive applications.
3. Further, we will try to improve the chemical stability and crystallinity of the COFs by using new factors like hydrogen bonding, keto-enol tautomerization, etc.
4. By using different type of linker units, we would like to synthesize a crystalline covalent organic frame works.

References:

1. L. Wang, L. Wang, J. Zhao, T. Yan. *J. App. Phys.* **2012**, *111*, 1126.
2. A. P. Côté, A. I. Benin, N. W. Ockwig, M. O'Keeffe, A. J. Matzger, O.M. Yaghi, *Science* **2005**, *310*, 1166.
3. H.M.El-Kaderi, Hunt, J.R. Mendoza-Cortés, J.L. Côté, A.P. Taylor, R.E. O'Keeffe, M. O.M. Yaghi, *Science* **2007**, *316*, 268.
4. O.M.Yaghi, M.O'Keeffe, N.W.Ockwig, H.K.Chae, M.Eddaoudi Kim. *J. Nature* **2003**, *423*, 705.
5. X.Feng, X.Ding, D.Jiang. *Chem. Soc. Rev.* **2012**, *41*, 6010.
6. J. W. Colson, A. R. Woll, A. Mukherjee, M. P. Levendorf, E. L. Spitler, V. B. Shields, M. G. Spencer, J. Park and W. R. Dichtel, *Science*, **2011**, *332*, 228.
7. P. Kuhn, M. Antonietti and A. Thomas, *Angew. Chem., Int. Ed.*, **2008**, *47*, 3450.
8. M. J. Bojdys, J. Jeromenok, A. Thomas and M. Antonietti, *Adv. Mater.*, **2010**, *22*, 2202.
9. N. L. Campbell, R. Clowes, L. K. Ritchie and A. I. Cooper, *Chem. Mater.*, **2009**, *21*, 204.
10. M. Dogru, A. Sonnauer, A. Gavryushin, P. Knochel and T. Bein, *Chem. Commun.*, **2011**, *47*, 1707.
11. S.-Y. Ding, X.-H. Cui, Y.-X. Ma and W. Wang, *Chem. Soc. Rev.*, **2013**, *42*, 548.
12. E. Tylianakis, E. Klontzas and G. E. Froudakis, *Nanoscale*, **2011**, *3*, 856.
13. Y. J. Choi, J. W. Lee, J. H. Choi and J. K. Kang, *Appl. Phys. Lett.*, **2008**, *92*, 173102.
14. M. M. Wu, Q. Wang, Q. Sun, P. Jena and Y. Kawazoe, *J. Chem. Phys.*, **2010**, *133*, 154706.
15. J.-T. Yu, Z. Chen, J. Sun, Z.-T. Huang and Q.-Y. Zheng, *J. Mater. Chem.*, **2012**, *22*, 5369.
16. Y. Li and R. T. Yang, *AIChE J.*, **2008**, *54*, 269.
17. H. Furukawa and O. M. Yaghi, *J. Am. Chem. Soc.*, **2009**, *131*, 8875.
18. K. Sumida, D. L. Rogow, J. A. Mason, T. M. McDonald, E. D. Bloch, Z. R. Herm, T.-H. Bae and J. R. Long, *Chem. Rev.*, **2012**, *112*, 724.
19. C. J. Doonan, D. J. Tranchemontagne, T. G. Glover, J. R. Hunt and O. M. Yaghi, *Nat. Chem.*, **2010**, *2*, 235.
20. S. Wan, J. Guo, J. Kim, H. Ihee and D. Jiang, *Angew. Chem., Int. Ed.*, **2008**, *47*, 8826.
21. I. Berlanga, M. Luisa Ruiz-Gonzalez, J. Maria Gonzalez- Calbet, J. L. G. Fierro, R. Mas-Balleste and F. Zamora, *Small*, **2011**, *7*, 1207.
22. S.-Y. Ding, J. Gao, Q. Wang, Y. Zhang, W.-G. Song, C.-Y. Su and W. Wang, *J. Am. Chem. Soc.*, **2011**, *133*, 19816.
23. X. Feng, L. Chen, Y. Dong and D. Jiang, *Chem. Commun.*, **2011**, *47*, 1979.

24. S. Wan, F. Gandara, A. Asano, H. Furukawa, A. Saeki, S. K. Dey, L. Liao, M. W. Ambrogio, Y. Y. Botros, X. Duan, S. Seki, J. F. Stoddart and O. M. Yaghi, *Chem. Mater.*, **2011**, 23, 4094.
25. X. Feng, L. Liu, Y. Honsho, A. Saeki, S. Seki, S. Irle, Y. Dong, A. Nagai and D. Jiang, *Angew. Chem., Int. Ed.*, **2012**, 51, 2618.
26. X. Ding, J. Guo, X. Feng, Y. Honsho, J. Guo, ; S. Seki, P. Maitarad, A. Saeki, S. Nagase, D. Jiang, *Angew. Chem., Int. Ed.* **2011**, 50, 1289;
27. Yue-Biao Zhang, Jie Su, Hiroyasu Furukawa, Yifeng Yun, Felipe Gándara, Adam Duong, Xiaodong Zou, and Omar M. Yaghi, *J. Am. Chem. Soc.* **2013**, 135, 16336.
28. Tonia Kretz, Jan Willem Bats, Hans-Wolfram Lerner, and Matthias Wagner *Z. Naturforsch.* **2007**, 62b, 66.
29. Sharath Kandambeth, Digambar Balaji Shinde, Manas K. Panda, Binit Lukose, Thomas Heine and Rahul Banerjee *Angew. Chem. Int. Ed.*, **2013**, 52, 13052.

Presented Poster on COFs

Covalent organic frameworks (COFs)



Rahul Raya D B Shinde and Rahul Banerjee*

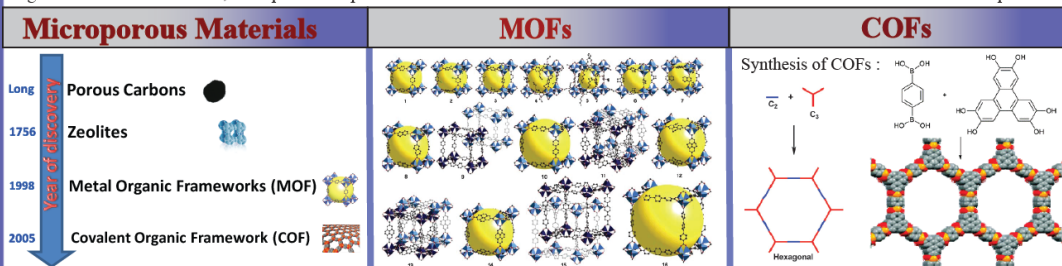
Physical/Materials Chemistry Division, National Chemical Laboratory,
Dr. Homi Bhabha Road, Pune-411008, India.

E-mail: rahul_raya@students.iiserpune.ac.in, db.shinde@ncl.res.in, r.banerjee@ncl.res.in

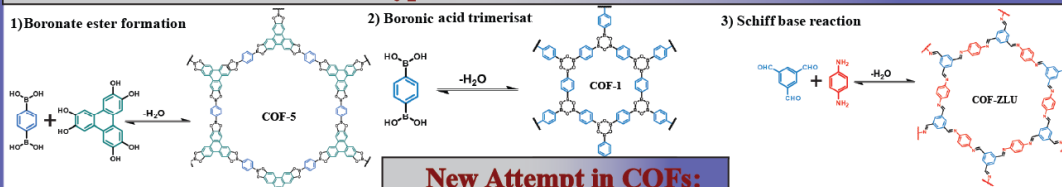


Abstract:

Covalent organic frameworks (COFs) represent an exciting new type of porous organic materials, which are ingeniously constructed with organic building units via strong covalent bonds. The well-defined crystalline porous structures together with tailored functionalities have offered the COF materials superior potential in diverse applications, such as gas storage, adsorption, optoelectricity, and catalysis. Since the seminal work of prof. Yaghi and co-workers in 2005, the rapid development in this research area has attracted intensive interest from researchers with diverse expertise.



Different types of COF formation reactions:



New Attempt in COFs:

<p>Stability problem in COFs:</p>	<p>Step-1: Crystallization of COF</p> <p>Reversible Schiff base reaction</p> <p>Enol form ↔ Keto form</p> <p>Irreversible tautomerism</p> <p>Step-2: Enhances chemical stability</p> <p>The total reaction scheme can be divided in to 2 steps. Step-1 is reversible and the reversibility in reaction helps the system to achieve the thermodynamically stable ordered crystalline structure. Step-2 is the irreversible tautomerism leads to the formation of highly stable keto form. The irreversibility in tautomerism will not effect the crystallinity because the atomic position remains same in both the cases.</p>	<p>COFs for Catalysis:</p> <p>First Principles Molecular Simulation</p>
--	--	--

Summary:

- 1) The covalent organic frameworks (COFs) represent a fascinating new type of crystalline porous materials. the COF materials possess the advantages of low density, large surface area, tunable properties and functionality because of versatile covalent-bonding of organic building units consisting of light elements (C, Si, O, B and N) only. the regular pore structures have offered the COF materials with superior potentials in advanced applications.
- 2) First time introduced a new protocol for the synthesis of highly acid and base stable crystalline covalent-organic frameworks.

Reference:

- 1) S. Kandambeth, A. Mallick, B. Lukose, M. V. Mane, T. Heine and R. Banerjee, *J. Am. Chem. Soc.*, 2012, 134, 19524–19527.
- 2) Côté, A. P.; Benin, A. I.; Ockwig, N. W.; Matzger, A. J.; O’Keeffe, M.; Yaghi O. M. *Science* 2005, 310, 1166
- 3) Shun Wan, Jia Guo, Jangbae Kim, Hyotcherl Ihee, and Donglin Jiang *Angew. Chem.* 2008, 120, 8958–8962
- 4) San-Yuan Ding, Jia Gao, Qiong Wang, Yuan Zhang, Wei-Guo Song, Cheng-Yong Su, and Wei Wang, *J. Am. Chem. Soc.* 2011, 133, 19816–19822

Financial Support:

Inspire (DST),
IISER pune,
NCL.
(Dr. Rahul Banerjee.)

THE END